IDENTIFICATION, STABILITY ANALYSIS AND CONTROL OF LINEAR TIME PERIODIC SYSTEMS VIA HARMONIC TRANSFER FUNCTIONS

A THESIS SUBMITTED TO

THE GRADUATE SCHOOL OF ENGINEERING AND SCIENCE

OF BILKENT UNIVERSITY

IN PARTIAL FULFILLMENT OF THE REQUIREMENTS FOR

THE DEGREE OF

MASTER OF SCIENCE

IN

ELECTRICAL AND ELECTRONICS ENGINEERING

By

Elvan Kuzucu Hıdır

August 2017

IDENTIFICATION, STABILITY ANALYSIS AND CONTROL OF LINEAR TIME PERIODIC SYSTEMS VIA HARMONIC TRANSFER FUNCTIONS

By Elvan Kuzucu Hıdır

August 2017

We certify that we have read this thesis and that in our opinion it is fully adequate, in scope and in quality, as a thesis for the degree of Master of Science.

Ömer Morgül (Advisor)

Arif Bülent Özgüler

Mehmet Önder Efe

Approved for the Graduate School of Engineering and Science:

Ezhan Karaşan
Director of the Graduate School

ABSTRACT

IDENTIFICATION, STABILITY ANALYSIS AND CONTROL OF LINEAR TIME PERIODIC SYSTEMS VIA HARMONIC TRANSFER FUNCTIONS

Elvan Kuzucu Hıdır
M.S. in Electrical and Electronics Engineering
Advisor: Ömer Morgül
August 2017

Many important systems encountered in nature such as wind turbines, helicopter rotors, power networks or nonlinear systems which are linearized around periodic orbit can be modeled as linear time periodic (LTP) systems. Such systems have been analyzed and discussed from analytical viewpoint extensively in the literature. However, only a few method are available in the literature for the identification of LTP systems which utilize input/output measurements. Especially, due to obtaining analytical solutions for LTP systems are quite challenging, utilization of experimental data to identify, analyze and stabilize such systems may be preferable. To achieve this aim, the utilization of harmonic transfer functions (HTFs) of LTP systems can be quite helpful.

In the first part of this thesis, we aim to obtain harmonic transfer functions (HTFs) of LTP systems via data-driven approach by using only input and output data of the system. In this respect, we first present the identification procedure of HTFs by using single cosine input signal with a specific frequency. However, because of the fact that this method requires multiple experiments in order to cover desired frequency range, we propose a formula for the sum of cosine input signal including different frequencies which their output components do not coincide. Then, we present the prediction performance of the estimated HTFs by using single cosine and sum of cosine input signals according to analytical solution of HTFs.

In the second part of the thesis, our goal is to utilize harmonic transfer functions in order to analyze and design controllers which stabilize and enhance the performance of LTP systems. In this regard, we implement well known Nyquist

stability criterion which is based on eigenloci of HTFs. As an illustrative example, we consider the well-known (unstable) damped Mathieu equation and design P, PD and PID controllers by using obtained Nyquist diagram.

Finally, for the unknown LTP systems whose state space model may not be available, we seek to design a novel methodology, where we can obtain Nyquist plots of unknown LTP systems via input-output data analysis using the concept of HTFs. Then, we design PD controllers for the unknown LTP system by using Nyquist diagram in order to enhance the performance and increase the robustness. We illustrate the performance results of these controllers in time domain simulations.

Keywords: Linear Time Periodic Systems, Harmonic Transfer Functions, Stability Analysis, PD Controllers, Nyquist Diagrams.

ÖZET

DOĞRUSAL VE ZAMANLA PERİYODİK OLARAK DEĞİŞEN SİSTEMLERİN HARMONİK TRANSFER FONKSİYONLAR YOLUYLA TANILANMASI, KARARLILIK ANALİZİ VE KONTROLÜ

Elvan Kuzucu Hıdır
Elektrik ve Elektronik Mühendisliği, Yüksek Lisans
Tez Danışmanı: Ömer Morgül
Ağustos 2017

Rüzgar türbinleri, helikopter rotorları, güç ağları veya periyodik yörünge çevresinde doğrusallaştırılmış doğrusal olmayan sistemler gibi doğada karşılaşılan birçok önemli sistem doğrusal ve zamanla periyodik değişen (DZPD) sistemler olarak modellenebilir. Bu tür sistemler literatürde analitik bakış açısıyla yoğun bir şekilde analiz edilmiş ve tartışılmıştır. Ancak, literatürde LTP sistemlerin tanımlanması için giriş / çıkış ölçümlerini kullanan sadece birkaç yöntem mevcuttur. Özellikle, LTP sistemleri için analitik çözümler elde etmek zor olduğu için, bu tür sistemleri tanılamak, analiz etmek ve kararlı hale getirmek için deneysel verilerin kullanılması tercih edilebilir olmaktadır. Bu amaca ulaşmak için, LTP sistemlere ait harmonik transfer fonksiyonlarının kullanılması oldukça yararlı olabilmektedir.

Bu tezin ilk bölümünde, sistemin sadece girdi ve çıktı verilerini kullanarak veri odaklı yaklaşımla DZPD sistemlerin harmonik transfer fonksiyonlarının elde edilmesi amaçlanmıştır. Bu bağlamda, önce belirli bir frekansa sahip tek kosinüs giriş sinyalini kullanarak HTF'lerin tanımlama prosedürünü sunulmuştur. Bununla birlikte, bu yöntem, istenen frekans aralığını karşılamak için çoklu deney yapılmasını gerektirdiği için, çıkış bileşenleri birbirine denk gelmeyen farklı frekansları içeren kosinüs giriş sinyalinin toplamı için bir formül önerilmiştir. Daha sonra, teorik HTF'lere göre tekli kosinüs ve kosinüs giriş sinyalleri toplam formülü kullanılarak tahmin edilen HTF'lerin tahmin performansını sunulmuştur.

Tezin ikinci bölümünde ise, DZPD sistemleri incelemek amacıyla ve performanslarını geliştirecek ve de sistemleri kararlı hale getirecek kontrolcüler tasarlamak için harmonik transfer fonksiyonlarından yararlanılmıştır. Bu bağlamda, kararsız sönümlü Mathieu denklemi için HTF özniteliklerine dayanarak elde edilen Nyquist kararlılık kriteri uygulanmış ve de Nyquist diyagramı kullanılarak P, PD ve PID kontrolcüler tasarlanmıştır.

Son olarak, durum uzayı modeli bulunmayan ve bilinmeyen DZPD sistemler için, HTF kavramını kullanarak girdi-çıktı veri analizi yoluyla bilinmeyen DZPD sistemlerin Nyquist grafiklerinin elde edebileceği yeni bir metodoloji tasarlanmaya çalışılmıştır. Ardından performansı geliştirmek ve gürbüzlüğü artırmak amacıyla Nyquist diyagramı kullanılarak bilinmeyen bir DZPD sistem için PD kontrolcüler tasarlanmıştır. Bu kontrolcülerin performans sonuçları zaman bölgesi benzetim ortamı testleriyle gösterilmiştir.

Anahtar sözcükler: DZPD Sistemler, Harmonik Transfer Fonksiyonları, Kararlılık Analizi, PD Kontrölcüler, Nyquist Diagramları.

Acknowledgement

Firstly, I would like to thank my supervisor, Ömer Morgül, for his guidance, encouragement and continuous support throughout my study. I feel very fortunate to be one of his students. He always encouraged and guided me through the learning process of my graduate education.

I am hugely thank İsmail Uyanık for inspiring me to the world of system identification. He always encourage me and he always there to listen and to give advice when I needed.

I would like to thank the distinguished members of my thesis jury Bülent Özgüler and Mehmet Önder Efe for approving my work and guiding me all the way up to this point. I am also indebted to all my instructors in undergraduate and graduate study in Bilkent. Especially, I would like to thank two of my amazing professors Hitay Özbay and Orhan Arıkan for their supports and guidance.

The members of my senior project group, HIDAR-3D; Dilan Öztürk, Bengisu Özbay, Mustafa Gül and Mansur Arısoy have contributed immensely to my personal and academic life. Thanks to them, we have achieved many excellent jobs and we have had an amazing year together. I want to thank especially Dilan Öztürk who was always with me every aspect of my life during six years. We had a great time at Bilkent.

Additionally, I am very thankful to the members of our research group Caner Odabaş, Ali Nail İnal, Hasan Hamzaçebi, Bahadır Çatalbaş, Eftun Orhon, Ahmet Safa Öztürk and Deniz Kerimoğlu. They always helped me along the way.

Outside the laboratory, there are some friends who directly or indirectly contributed to completion of my thesis. I am grateful to mu friends Serkan Sarıtaş, Ersin Yar and Ahmet Dündar Sezer. I would also like to express my sincere gratitude to Hayrunnisa Altın. She was always there to listen and motivate me.

I want to thank Mürüvet Parlakay and Aslı Tosuner for their helps on administrative works and Ergün Hırlakoğlu, Onur Bostancı and Ufuk Tufan for their technical support.

I am appreciate of financial support from the Scientific and Technological Research Council of Turkey (TÜBİTAK).

Finally but forever, I owe my loving thanks to my husband Ahmet Sadık Hıdır for his unconditional love. I am indebted to my parents Emine - Fikret Kuzucu and Bedia - Mehmet Nil Hıdır and my lovely sisters Nazmiye, Ceyda and Çiğdem for their undying love, support and encouragement in my whole life.

Contents

List of Figures

List of Tables

to my parents and to my beloved husband

Chapter 1

Introduction

1.1 Motivation and Background

Many significant systems should be modeled with linear time periodic equations of motion in order to provide successful stability analysis and control tools for these systems. Examples of such systems include wind turbines [1–3], helicopter rotors [4–7] and some nonlinear systems linearized around a periodic trajectory [8–11]. Note that the modeling of these systems as linear time invariant (LTI) generally does not represents the behavior of the systems correctly. For instance; switching nature of power networks results with harmonics. For traditional power systems which include a few harmonics, it is stated that harmonics does not affect the stability of network. However, with the increasing number of switched components, harmonics have to be considered in order to guarantee stability of power networks which requires consideration of linear time periodic systems analysis methods [12].

In order to model and describe input output relation of linear time periodic (LTP) systems, a linear operator based method (Harmonic Transfer Functions) is

developed in [13]. For LTP systems, many different system identification methods are proposed in time domain and frequency domain. State space identification and discrete-time identification methods are proposed in [14–18]. However, sometimes frequency domain identification methods can be more preferable to understand the structure of sophisticated LTP systems [19]. In this respect, the identification methodology in frequency domain is established by using power and cross spectral density functions in [6]. Also, in [5], a similar strategy is developed by adding a noise signal to the input and output signals. As a result of the identification procedure in frequency domain, the harmonic transfer functions consists of multiple modulated LTI transfer functions which describe the relation between any harmonics of LTP system in the output signal and input signal. This is because, unlike LTI systems, if sinusoidal input with a specific frequency is applied to the LTP system, the system generates an output signal which includes different harmonics of frequencies of the system.

On the other hand, in addition to the identification problem, harmonic transfer functions can be utilized in various aspects of LTP systems. Because of the fact that LTI systems can be represented with a single transfer function, modeling, stability analysis or control of these systems is simple in frequency domain via estimated transfer function. However, with these techniques it is usually difficult to perform a parametric stability analysis. In this respect, Nyquist stability criterion based on eigenloci of harmonic transfer functions is developed in order to analyze stability of LTP systems in frequency domain [20] which is similar to the stability criterion of multi-input multi-output systems via transfer function.

Stability of LTP systems can be investigated via Floquet theory by examining the eigenvalues of their corresponding monodromy matrix which can be hard to find or Lyapunov theory can be also used. However, these techniques has suffered from similar restriction which is to give yes or no answer to the stability question of LTP systems when all parameters of the system are fixed [21]. If there is a feedback in the system, closed loop stability analysis requires effort with these methods since stability is determined for a single value of feedback. However, thanks to the Nyquist diagram which is obtained by using eigenloci of HTF, closed loop stability analysis can be specified for a gain parameter family.

Another purpose of the use of HTFs is the control of LTP systems in frequency domain in order to stabilize and enhance the performance. Many controller design methodologies for LTP systems are developed based on state space model. Linear quadratic regulator (LQR) is a well known controller which is used in control of many LTP systems; especially for attenuating helicopter vibrations [7, 22, 23]. The objective of LQR problem is to design a full state feedback law which minimizes the quadratic cost function. LQR gain is obtained by using the solution of a differential Riccati equation. It is an optimal controller and provides periodic feedback gains which improve the robustness of the system while guaranteeing the closed loop stability. However, to obtain optimal feedback gain, solution of differential Riccati equation requires the knowledge of state matrices of LTP system. In the case where state space model of LTP is unknown and only harmonic transfer functions are known, designing a controller can become a challenging problem. Using the Nyquist criterion which is based on eigenloci of HTFs, a static feedback gain controller can be designed that guarantees closed loop stability. On the other hand, designing constant feedback controller may not be sufficient the specific stability robustness properties such as gain and phase margins. For this purpose, as integrating harmonic transfer function structure of proportional derivative (PD) controller to the harmonic transfer function of plant, Nyquist criterion can be applied. Then, considering robustness and stability issues, parameters of the controller can be designed to obtain a closed loop system, which is stable and has acceptable performance.

Motivated by these problems, we primarily present a methodology for system identification of LTP systems which may identify the system correctly by using only input and output data. We first use single cosine input signal to excite the system and by investigating input-output relation for each frequencies separately, we perform the identification procedure. Since covering all frequencies requires multiple experiments, we develop a formula for sum of cosine input signal, which includes many different cosine signals at various frequencies which their outputs do not coincide. After we obtain harmonic transfer functions of LTP systems, we analyze the stability of the system via Nyquist criterion which is based on eigenloci of HTFs. In order to stabilize and enhance the performance of these

systems, we design feedback gain and PD, PID controllers by using theoretically derived and estimated harmonic transfer functions. After that, we show how to enhance the performance and stability robustness of LTP system by using estimated HTFs in the case where only input and output data of the system is known.

1.2 Existing Work

A linear operator that defines the relation between input and output of LTP systems is presented as harmonic transfer functions in [13]. Identification of harmonic transfer functions of the systems plays a crucial role in order to analyze stability and control of LTP systems. Many of these methods characterize the LTP systems analytically and making system identification based on measurements take less attention accordingly. Existing studies on experimental system identification of LTP systems is developed in [6] by using power and cross spectral density functions. The strategy which is analogous to [6] is developed in [5] to identify harmonic transfer functions by considering the noise in input and output measurements. Another identification method is used in [8] for identifying models of nonlinear systems by using linearization around their periodic orbits and approximating the system as LTP. For this purpose, lifting method is used with the Algorithm of Mode Isolation.

For the stability analysis of LTP systems, Floquet theory is available [24]. The theory consists of examining the eigenvalues of fundamental monodromy matrix of LTP systems. Stability analysis can also be achieved with Lyapunov theory [25] or Hill determinant methodology [26]. However, these techniques suffer from answering closed loop stability question of LTP systems for only a specific value of feedback gain. Nyquist criterion based on eigenloci, which consists of circuits of eigenvalues of harmonic transfer functions, is developed in [20]. When the feedback gain is applied to the output of LTP systems, Nyquist stability criterion provides determination of closed loop stability for a family of gain parameters. Another advantage of Nyquist criterion is that even if one does not know the state

space model of the LTP systems, stability analysis can be achieved via Nyquist diagram of estimated harmonic transfer functions.

For the control of LTP systems, many different methodologies are developed. One of the most significant control strategy among these is linear quadratic regulator (LQR) controller because of providing periodic feedback gain which guarantees stability and robustness [27, 28]. LQR controller is favorable especially for the control of active vibrations in LTP systems such as wind turbines, helicopter rotors or turbo-machinery [7, 22]. In order to design optimal state feedback gain via LQR, we have to know the state space model of the LTP system. However, for the case which the system is unknown, control of LTP systems can be provided by Nyquist criterion via harmonic transfer functions. To control LTP systems, static feedback gain controller is designed by using Nyquist diagram in [13]. Also, stability analysis and control of power network systems is achieved in [29–31] by using theoretically derived harmonic transfer functions.

1.3 Methodology and Contribution

In addition to the stability analysis and control of the LTP systems, analytical and experimental identification play a crucial role in order to characterize them properly. Although there are many different system identification strategies in time domain, frequency domain identification approaches can be preferred in many times when it is difficult to model complex LTP systems. In this respect, we first develop an identification procedure by using single cosine input signal with a specific frequency and measuring its corresponding output signal. By dividing Fourier transform of the output to the Fourier transform of input signal, transfer function is obtained at the input frequency. However, in order to recover desired frequency range, multiple experiment has to be done. For this reason, we first design an input signal which consists of sum of cosine input signal at various frequencies which their corresponding output harmonic components do not coincide. Hence, we provide frequency domain system identification procedure with a few experiments in a systematic way.

In the second part, we investigate the methodology for stability analysis and control of LTP systems by using harmonic transfer functions. In this regard, we implement the well known Nyquist stability criterion which is based on eigenloci of harmonic transfer functions in order to analyze the stability of LTP systems. For the case in which a feedback gain is applied to the output of LTP systems, stability analysis can be performed for a family of gain parameters. To demonstrate these ideas, we consider the well known damped Mathieu example which exhibits both stable and unstable behaviors in certain parameter ranges. Hence, for the unstable LTP example, the range for the feedback gain which stabilize the system is obtained by using Nyquist stability test. Even though static feedback is sufficient to stabilize unstable LTP system, it does not enhance the performance of the systems in terms of robustness issue which is very significant to obtain successful controllers especially for unmodeled systems. Because of that reason, we design a PD and PID controllers in order to both stabilize and enhance the performance of the system. In designing K_p parameters of these controllers as feedback gain and integrating harmonic transfer functions of these controllers to the harmonic transfer function of the plant, we plot Nyquist diagram and apply Nyquist stability criterion. As a result of this criterion, we obtain the stability range for family of K_p parameter instead of analyzing the stability for only a single value of K_p. By obtaining gain and phase margins of the close loop system from the Nyquist diagram, we design a robust and stabilized controllers.

In the final part, without knowing state space model of the LTP systems, we first achieve system identification and obtain harmonic transfer function of the system by using only input and output data. An important point here is that we assume the stability of this system in order to use input and output data, otherwise output data will be meaningless. Then, in order to enhance the performance of LTP system, we design a robust and stable controller by using Nyquist diagram of estimated harmonic transfer function via sum of cosine input signal and its corresponding outputs.

1.4 Organization of Thesis

In the first part of the thesis, we give preliminary information about linear time periodic systems in order to understand the structure of them. After providing significant results of Floquet theory, analytical solution of harmonic transfer functions is illustrated which present input and output relation of LTP systems. In Chapter 3, we illustrate data-driven approaches in order to identify LTP systems in frequency domain. In this respect, we give the identification methodology of [6] which uses chirp input signal to excite the system. Then, we show the identification procedure for the single cosine input signal and we propose a formula for the input signal which includes sum of different cosine signals and we guarantee that their corresponding outputs do not coincide. Finally, we compare the estimation performance of these methods with theoretical harmonic transfer function for simple legged robot model.

In Chapter 4, we illustrate the use of harmonic transfer functions for the stability analysis and control of LTP systems. We illustrate the Nyquist diagram of LTP systems via eigenloci of harmonic transfer functions. Then, analysis of stability from the Nyquist diagram is demonstrated. Use of estimated harmonic transfer functions in order to obtain Nyquist diagram is also explained. After we give the algorithm for the controller design based on harmonic transfer functions, for unstable lossy Mathieu example P, PD and PID controllers are designed. Robustness properties of the closed loop system with controller are plotted in terms of gain and phase margins by using Nyquist diagram. By using the designed controller, time domain simulations are presented and performance of the system is investigated in terms of percentage overshoot, settling time and etc. Finally, we apply the Nyquist criterion by using estimated harmonic transfer function and design controllers which enhance the performance for the stable lossy Mathieu equation.

We conclude the thesis with Chapter 5 which includes final remarks and future extensions of this study.

Chapter 2

Linear Time Periodic Systems

Time-dependent periodic system dynamics are frequently confronted in nature and in engineering applications. Wind turbines [3], rotor tilt systems [32], power distribution networks [31], and walking / running behaviors of human and animals [14, 33] are examples of periodic systems that are frequently confronted and increasingly used. The increase in the rate of use of periodic systems has also led to development in the analysis, system identification and control of such systems [13, 14, 34, 35]. The main objective of this chapter is firstly to give some mathematical preliminaries about Linear Time Periodic (LTP) Systems which is required for the study of these systems. Secondly, we explain the Floquet theory and its analysis tools which have been widely used in the study of LTP systems. Finally, we provide information about Harmonic Transfer Functions (HTF) describing transfer properties of LTP systems, which is analogous to LTI transfer functions [36].

2.1 Mathematical Preliminaries

2.1.1 Overview of Linear Time Invariant (LTI) Systems

State-space representations of LTI systems are shown as

$$\begin{aligned} \dot{x}(t) &= Ax(t) + Bu(t) \\ y(t) &= Cx(t) + Du(t) \end{aligned} \tag{2.1}$$

where $x \in \mathbb{R}^{n}$ is the state vector, $u \in \mathbb{R}^{m}$ is the input vector and $y \in \mathbb{R}^{p}$ is the output vector. $A \in \mathbb{R}^{n\times n}$, $B \in \mathbb{R}^{n\times m}$, $C \in \mathbb{R}^{p\times n}$ and $D \in \mathbb{R}^{m\times p}$ are constant matrices.

By taking Laplace transform of (2.1) with $x(0) = 0$ and by eliminating the state variable we obtain

$$Y(s) = G(s)U(s) \tag{2.2}$$

where the transfer function $G(s)$ is given as

$$G(s) = C(sI - A)^{-1}B + D. \tag{2.3}$$

where I represents the identity matrix with appropriate dimension.

2.1.2 Linear Time Periodic (LTP) Systems

Characterization of LTP systems is more difficult than LTI systems since differential equation's coefficients which define the system dynamics of LTP systems are periodic and time-varying. State space representation of an LTP system is in the form

$$\begin{aligned} \dot{x}(t) &= A(t)x(t) + B(t)u(t) \\ y(t) &= C(t)x(t) + D(t)u(t) \end{aligned} \tag{2.4}$$

where for each $t \in \mathbb{R}^{+}$, $A(t) \in \mathbb{R}^{n\times n}$, state matrix, $B(t) \in \mathbb{R}^{n\times m}$, $C(t) \in \mathbb{R}^{p\times n}$ and $D(t) \in \mathbb{R}^{n\times n}$ are all T periodic, i.e.,

$$A(t + NT) = A(t), \tag{2.5}$$

for any integer value of N and it is similar for B, C and D. Here $T > 0$ is the minimum constant real number satisfying (2.5), which is called as fundamental period. $x(t) \in \mathbb{R}^n$ is state vector, $u(t) \in \mathbb{R}^m$ is control vector and $y(t) \in \mathbb{R}^m$ is the output vector. A brief notation of the state space model, S, of the LTP system is given in [36] as,

$$S = \left[\begin{array}{c|c} A(t) & B(t) \\ \hline C(t) & D(t) \end{array}\right]. \tag{2.6}$$

If $D(t) \equiv 0 \; \forall t$, S will be called as strictly proper. The fundamental frequency or pumping frequency of LTP system is defined by

$$\omega_0 = 2\pi/T \tag{2.7}$$

If we apply a complex exponential or a sinusoidal input signal with a specific frequency, ω, to excite the LTP system, then the output generates superposition of input signals at input frequency, ω, and also at other frequencies, $\omega + n\omega_0$ with possibly different magnitude and phase [36]. Here, $n\omega_0$ represents the harmonics of the fundamental frequency and the frequencies, $\omega + n\omega_0$, are generally referred to as harmonics.

2.2 Floquet Theory

Floquet theory has played an important role in studying the LTP systems and provides several significant results [24]. The Floquet theory has been used in many different areas such as stability analysis of helicopter rotor blade dynamics and power systems [12, 37] or identification of legged locomotion systems [38]. The main objective of Floquet analysis is to transform the LTP system given by (2.4) to an equivalent LTP system (with a T-periodic linear transformation) the state matrix A of which becomes a constant matrix.

Let $\Phi(t, \tau)$ be the state transition matrix of (2.4). The fundamental monodromy matrix of (2.4) is denoted as $\Phi(T, 0)$.

Theorem 2.2.1. *[24] If fundamental monodromy matrix, $\Phi(T,0)$, of tan LTP system defined is nonsingular, then following results hold:*

1. **State transition matrix:** State transition matrix of LTP system in (2.6) can be expressed as [40]:

$$\Phi(t,0) = P(t)e^{\bar{A}t}$$

where $P(t) \in \mathbb{R}^{n\times n}$ is a T-periodic matrix: $P(t) = P(t+T)$ and $\bar{A} \in \mathbb{R}^{n\times n}$ is constant matrix (possibly with complex entries).

2. **Similarity Transform:** The transformation $x = P(t)z$ transforms (2.6) to the following equivalent as

$$\begin{aligned} \dot{z}(t) &= \bar{A}z(t) + \bar{B}(t)u(t) \\ y(t) &= \bar{C}(t)z(t) + \bar{D}(t)u(t) \end{aligned} \tag{2.8}$$

where

$$\begin{aligned} \bar{A} &= P^{-1}(t)(A(t)P(t) - \dot{P}(t)) \\ \bar{B}(t) &= P^{-1}(t)B(t) \\ \bar{C}(t) &= C(t)P(t) \end{aligned} \tag{2.9}$$

3. **Stability Analysis:** The LTP system given by (2.4) is stable if and only if all eigen values of the fundamental monodromy matrix are strictly inside the open unit disc, i.e. when the following holds:

$$\lambda\left\{\Phi(T,0)\right\} \in D_o \tag{2.10}$$

where $D_o = \left\{z| \quad |z| < 1\right\}$.

2.3 Harmonic Transfer Functions

In literature, there are many different system identification methods for the stable LTI systems due to one-to-one mapping between characteristics of input and

output signal's frequency response at steady state [14]. Hence, we can easily obtain frequency response functions of LTI systems including magnitude and phase diagrams of output signal with respect to input signal. However, in LTP systems because of time dependency of system matrices, if one applies sinusoidal inputs, the response of the system contain multiple harmonics possibly each with different magnitude and phase. In order to obtain one-to-one mapping as in LTI systems, ignoring all of the high order harmonics in the output can cause incorrect results.

As a remedy to this problem, Wereley developed an alternative approach by transforming input and output signals of LTP systems to exponentially modulated periodic (EMP) signals [13]. To describe input-output relations of LTP systems, EMP signals are suitable which provide one-to-one mapping for modulated Fourier Series coefficients for EMP signals of input and output signals of LTP system. Thus, by using EMP signals, it is possible to obtain an input/output relation which is called as harmonic transfer functions.

2.3.1 Representation of Input-Output Relation of LTP Systems via Exponentially Modulated Signals

The results given in [13] shows that if an exponentially modulated periodic (EMP) signal is applied to the LTP system , the output and the state responses are also EMP signals at steady state. Hence, the output response represents transfer function concept for LTP system by providing a one-to-one mapping between EMP input signal and EMP output signal.

To represent relationship between input and output of LTP system, let us assume that the input signal is given as an EMP signal as given below:

$$u(t) = \sum_{n \in Z} u_n e^{s_n t}. \tag{2.11}$$

Then, the state vector can also be written as an EMP signal as given below,

$$\begin{aligned} x(t) &= \sum_{n\in Z} x_n e^{s_n t}, \\ \dot{x}(t) &= \sum_{n\in Z} s_n x_n e^{s_n t}. \end{aligned} \tag{2.12}$$

Similarly the output signal, $y(t)$ can also be written as an EMP signal as given below,

$$y(t) = \sum_{n\in Z} y_n e^{s_n t}, \tag{2.13}$$

where $s_n = s + jnw_0; \quad \forall n \in Z;\ s \in C$. The system matrices of LTP systems can be written in terms of complex Fourier series as,

$$A(t) = \sum_{n\in Z} A_n e^{jn\omega_0 t}, \tag{2.14}$$

Other matrices, $B(t)$, $C(t)$ and $D(t)$ can be written in a similar way as given below:

$$B(t) = \sum_{n\in Z} B_n e^{jn\omega_0 t}, \tag{2.15}$$

$$C(t) = \sum_{n\in Z} C_n e^{jn\omega_0 t}, \tag{2.16}$$

$$D(t) = \sum_{n\in Z} D_n e^{jn\omega_0 t}. \tag{2.17}$$

Then, by using these expansions in the (2.4), we obtain:

$$\begin{aligned} \sum_{n=-\infty}^{\infty} s_n x_n e^{s_n t} &= \sum_{n=-\infty}^{\infty} A_n e^{jn\omega_0 t} \sum_{m=-\infty}^{\infty} x_m e^{s_m t} + \sum_{n=-\infty}^{\infty} B_n e^{jn\omega_0 t} \sum_{m=-\infty}^{\infty} u_m e^{s_m t} \\ &= \sum_{n,m=-\infty}^{\infty} A_{n-m} x_m e^{s_n t} + \sum_{n,m=-\infty}^{\infty} B_{n-m} u_m e^{s_n t}. \end{aligned} \tag{2.18}$$

For the output in (2.4), similarly we obtain:

$$\sum_{n=-\infty}^{\infty} y_n e^{s_n t} = \sum_{n,m=-\infty}^{\infty} C_{n-m} x_m e^{s_n t} + \sum_{n,m=-\infty}^{\infty} D_{n-m} u_m e^{s_n t}. \tag{2.19}$$

By simplifying (2.18) and (2.19), we obtain:

$$\begin{aligned} 0 &= \sum_{n=-\infty}^{\infty} \underbrace{\left\{ s_n x_n - \sum_{m=-\infty}^{\infty} A_{n-m} x_m - \sum_{m=-\infty}^{\infty} B_{n-m} u_m \right\}}_{0} e^{s_n t}, \\ 0 &= \sum_{n=-\infty}^{\infty} \underbrace{\left\{ y_n - \sum_{m=-\infty}^{\infty} C_{n-m} x_m - \sum_{m=-\infty}^{\infty} D_{n-m} u_m \right\}}_{0} e^{s_n t}, \end{aligned} \tag{2.20}$$

The complex exponential terms in (2.20) form an orthonormal basis in $L_2[0,T]$ and hence, in order to satisfy (2.20), the terms inside the curl brackets in (2.20) should be equal to zero $\forall n \in Z$. Thus, we obtain the following equations:

$$\begin{aligned} s_n x_n &= \sum_{m=-\infty}^{\infty} A_{n-m} x_m - \sum_{m=-\infty}^{\infty} B_{n-m} u_m, \\ y_n &= \sum_{m=-\infty}^{\infty} C_{n-m} x_m - \sum_{m=-\infty}^{\infty} D_{n-m} u_m. \end{aligned} \tag{2.21}$$

We note that this is also called as harmonic balance in [13].

2.3.2 Toeplitz Transform of System Matrices

The equations in (2.21) provides comprehensible representation between Fourier coefficients of input-output signals. Alternatively, the infinite sum representation given by (2.21) can also be represented by a Toeplitz notation to represent infinite summations via matrix operations. Thus, the system equations in (2.21) can be written as doubly infinite matrix equation as follows

$$\begin{aligned} s\mathcal{X} &= (\mathcal{A} - \mathcal{N})\mathcal{X} + \mathcal{B}\mathcal{U}, \\ \mathcal{Y} &= \mathcal{C}\mathcal{X} + \mathcal{D}\mathcal{U}, \end{aligned} \tag{2.22}$$

Here, $\mathcal{U}(s)$, $\mathcal{Y}(s)$ and $\mathcal{X}(s)$ are input, output and state doubly infinite vectors respectively given in below:

$$\mathcal{U}(s) = [..., u_{-1}^T(s), u_0^T(s), u_1^T(s), ...]^T, \tag{2.23}$$

$$\mathcal{Y}(s) = [..., y_{-1}^T(s), y_0^T(s), y_1^T(s), ...]^T, \tag{2.24}$$

$$\mathcal{X}(s) = [..., x_{-1}^T(s), x_0^T(s), x_1^T(s), ...]^T. \tag{2.25}$$

where $u_n(s)$, $y_n(s)$, $x_n(s)$ corresponds to n^{th} harmonic component of $u(t)$, $y(t)$ and $x(t)$ respectively, and the superscript T represents the transpose.

T-periodic state matrix, $A(t)$ can be represented as doubly infinite block Toeplitz matrix in terms of its complex Fourier coefficients as the following Toeplitz form,

$$\mathcal{A} = \begin{bmatrix} \ddots & \vdots & \vdots & \vdots & \vdots & \\ \dots & A_0 & A_{-1} & A_{-2} & A_{-3} & \dots \\ \dots & A_1 & A_0 & A_{-1} & A_{-2} & \dots \\ \dots & A_2 & A_1 & A_0 & A_{-1} & \dots \\ \dots & A_3 & A_2 & A_1 & A_0 & \dots \\ & \vdots & \vdots & \vdots & \vdots & \ddots \end{bmatrix}, \tag{2.26}$$

$B(t)$, $C(t)$ and $D(t)$ matrices can be expressed as a doubly infinite Toeplitz matrix in terms of their corresponding complex Fourier coefficients similarly as follows:

$$\mathcal{B} = \begin{bmatrix} \ddots & \vdots & \vdots & \vdots & \vdots & \\ \dots & B_0 & B_{-1} & B_{-2} & B_{-3} & \dots \\ \dots & B_1 & B_0 & B_{-1} & B_{-2} & \dots \\ \dots & B_2 & B_1 & B_0 & B_{-1} & \dots \\ \dots & B_3 & B_2 & B_1 & B_0 & \dots \\ & \vdots & \vdots & \vdots & \vdots & \ddots \end{bmatrix}, \tag{2.27}$$

$$\mathcal{C} = \begin{bmatrix} \ddots & \vdots & \vdots & \vdots & \vdots & \\ \dots & C_0 & C_{-1} & C_{-2} & C_{-3} & \dots \\ \dots & C_1 & C_0 & C_{-1} & C_{-2} & \dots \\ \dots & C_2 & C_1 & C_0 & C_{-1} & \dots \\ \dots & C_3 & C_2 & C_1 & C_0 & \dots \\ & \vdots & \vdots & \vdots & \vdots & \ddots \end{bmatrix}, \tag{2.28}$$

$$\mathcal{D} = \begin{bmatrix} \ddots & \vdots & \vdots & \vdots & \vdots & \\ \dots & D_0 & D_{-1} & D_{-2} & D_{-3} & \dots \\ \dots & D_1 & D_0 & D_{-1} & D_{-2} & \dots \\ \dots & D_2 & D_1 & D_0 & D_{-1} & \dots \\ \dots & D_3 & D_2 & D_1 & D_0 & \dots \\ & \vdots & \vdots & \vdots & \vdots & \ddots \end{bmatrix}. \tag{2.29}$$

Another doubly infinite Toeplitz form matrix in (2.22) $\mathcal{N}$ is the modulation frequency matrix defined as follows:

$$\mathcal{N} = \begin{bmatrix} \ddots & \vdots & \vdots & \vdots & \\ \dots & -j\omega_0 I & 0 & 0 & \dots \\ \dots & 0 & 0 & 0 & \dots \\ \dots & 0 & 0 & j\omega_0 I & \dots \\ & \vdots & \vdots & \vdots & \ddots \end{bmatrix} \tag{2.30}$$

where I is identity matrix with same dimension as in the state matrix $A(t)$.

2.3.3 Harmonic State Space Model

The doubly infinite matrix equations in (2.22) is called as harmonic state space model and is expressed with $\widetilde{S}$ as:

$$\widetilde{S} = \left[\begin{array}{c|c} \mathcal{A}-\mathcal{N} & \mathcal{B} \\ \hline \mathcal{C} & \mathcal{D} \end{array}\right]. \tag{2.31}$$

In order to describe LTP systems, the harmonic state space model is very useful since it provides explicit relationship between Fourier coefficients of input and output. This relationship is achieved by the infinite dimensional matrix called as harmonic transfer functions (HTF), $\mathcal{H}(s)$, such that

$$\mathcal{Y}(s) = \mathcal{H}(s)\mathcal{U}(s). \tag{2.32}$$

At this point, HTFs can be obtained in terms of doubly infinite Toeplitz form of system matrices by isolating the terms input and output signals from (2.31) as:

$$\mathcal{H}(s) = \mathcal{C}[sI - (\mathcal{A}-\mathcal{N})]^{-1}\mathcal{B} + \mathcal{D}, \tag{2.33}$$

As a result, $\mathcal{H}(s)$ has doubly infinite dimensional matrix structure as given below:

$$\mathcal{H}(s) = \begin{bmatrix} \ddots & \vdots & \vdots & \vdots & \\ \dots & H_0(s-j\omega_0) & H_{-1}(s) & H_{-2}(s+j\omega_0) & \dots \\ \dots & H_1(s-j\omega_0) & H_0(s) & H_{-1}(s+j\omega_0) & \dots \\ \dots & H_2(s-j\omega_0) & H_1(s) & H_0(s+j\omega_0) & \dots \\ & \vdots & \vdots & \vdots & \ddots \end{bmatrix}. \tag{2.34}$$

As $H_0(s)$ is LTI transfer function which relates the input $u_0(s)$ to the dc output part of LTP system $y_0(s)$, $H_n(s)$ is also LTI transfer function that relates the input $u_0(s)$ at dc level to the n^{th} harmonic $y_n(s)$ of the output for $\forall n \in Z$. Thus, it shows us that the LTP harmonic transfer function is analogous to the LTI transfer function. However, the matrices shown in (2.22) are infinite dimensional. For computer simulations, we can truncate HTF. Generally, when number of harmonics increase, their values become smaller with respect to their order. Therefore, first few harmonics can be sufficient to describe LTP system with reasonable accuracy.

Chapter 3

System Identification of LTP Systems via Data-Driven Methods

In this chapter, we aim to present different methods to provide data-driven identification of LTP systems. In order to analyze and control LTP systems, harmonic transfer functions (HTFs) are one of the most significant tools. As frequency response of LTI systems produces an output at a specific frequency where input signal is applied, LTP systems generate output at frequencies seperated by a multiple of the fundamental frequency, ω_0, of the system. That is, there is coupling which can be described by HTFs between input and different harmonics of the output. Therefore, standard identification techniques of LTI systems cannot be applied to determine transfer functions of LTP systems. In this respect, we first overview the system identification of LTI systems. Then, we present identification strategy of [6] in order to estimate HTFs of LTP systems via exciting the system with chirp signals and using power and cross spectral density functions. Secondly, we show the single cosine method to identify HTFs of LTP system which requires multiple experiments to cover desired frequency range. Then, to estimate HTFs of LTP system, we propose a formula for exciting input signal which consists of sum of different cosine signals where harmonics of its outputs do not coincide.

Finally, we use these techniques in order to estimate HTFs of simplified vertical hopping robot model which is developed in [41] and compare estimation results of these methods with theoretical derivation of HTFs of this model.

3.1 Overview of System Identification of LTI Systems

Before we give the system identification method of [6], we review system identification and show empirical transfer function estimates of LTI systems [42]. In LTI systems, estimated transfer function, $\hat{G}(j\omega)$, is the ratio of Fourier transform of input and output such that,

$$\hat{G}(j\omega) = \frac{\mathcal{F}\left\{y(t)\right\}}{\mathcal{F}\left\{u(t)\right\}}, \tag{3.1}$$

where $\mathcal{F}$ represents the Fourier transform.

If there is a noise, $e(t)$, output will be in time domain as follows:

$$y(t) = \hat{g}(t) * u(t) + e(t), \tag{3.2}$$

where $\hat{g}(t)$ represents the estimated impulse response and $*$ denotes the convolution operation.

For stationary process, cross correlation between input and output, $R_{uy}(t)$, is given as:

$$\begin{aligned} R_{uy}(t) &= E[u(t)y(t+\tau)] \\ &= \int_0^\infty g(r)E[u(t)u(t+\tau-r)]dr + \int_0^\infty E[u(t)e(t+\tau-r)]dr \end{aligned} \tag{3.3}$$

If we assume that the noise, e, and input, u are independent random processes and have mean zero, second integral term in (3.3) is equal to zero and following holds:

$$\begin{aligned} R_{uy}(t) &= \int_0^\infty g(r)R_{uu}(\tau-r)dr \\ &= g(\tau) * R_{uu}(\tau) \end{aligned} \tag{3.4}$$

Then, if we take Fourier transform of this relation and convert it to frequency domain, we obtain the following:

$$S_{uy}(\omega) = \hat{G}(j\omega)S_{uu}(\omega) \tag{3.5}$$

where $S_{uy}(\omega)$ and $S_{uu}(\omega)$ are cross and power spectral density respectively. Then, estimated transfer function is equal to:

$$\hat{G}(j\omega) = \frac{S_{uy}(\omega)}{S_{uu}(\omega)} \tag{3.6}$$

3.2 Overview of System Identification of LTP Systems

In LTP systems, if one can provide state space representation or impulse response function of the system, theoretical derivation of harmonic transfer functions can be obtained by using the steps defined in Section 2.3. However, when the state space model of LTP system is unknown, the estimation of HTFs has great importance. Because of the fact that an input sinusoidal signal at single frequency produces an output as a superposition of sinusoids at different frequencies of diverse magnitudes and phases for LTP system, classical methods for identification of LTI systems are not adequate. Therefore, in this section, we introduce system identification methods for LTP systems.

3.2.1 System Identification with Chirp Input Signal

In this section, we review system identification method of [6] via chirp input signal. Before we illustrate this approach, initially some of the harmonic components at the output of LTP systems should be truncated. The reason for this is that the structure of HTF has infinite number of harmonics that can cause a problem for implementations on computer. Therefore, [6] suggests truncation of harmonics beyond a certain order and consider merely three frequencies at the output. Fundamental frequency of the system is ω_0 and output at any frequency ω consists of

linear combinations of the responses at frequencies, ω, $\omega + \omega_0$ and $\omega - \omega_0$ results with three harmonic transfer functions, $\hat{H}_0$, $\hat{H}_1$, and $\hat{H}_{-1}$ respectively. Then, the estimated output, $\hat{Y}$ can be represented as:

$$\begin{aligned}\hat{Y}(j\omega) := &\hat{H}_0(j\omega)U(j\omega) \\ &+ \hat{H}_1(j\omega)U(j\omega - j\omega_0) \\ &+ \hat{H}_{-1}(j\omega)U(j\omega + j\omega_0)\end{aligned} \tag{3.7}$$

Here, a component with $\hat{}$ is used in order to represent estimated version of harmonic transfer functions. The estimation problem of $\hat{H}_0$, $\hat{H}_1$, and $\hat{H}_{-1}$ can be formulated as the minimization of the difference between estimated and measured output of the system.

For identification process, selection of input signal plays an important role since there are three unknowns and only one equation. To solve this problem, [6] suggests to apply three identical inputs which are evenly spread out over system period and measure their corresponding outputs. In this respect, chirp signals can be used in order to obtain the frequency response of the system over a specific range of frequencies [6, 43]. The input chirp signal comprise of phase shifted replicas of original chirp signal which provides to be sure from evenly excitation of system throughout system period. An example for input chirp signal is shown in Fig. 3.1. The sample formula for chirp signal can be written as:

$$u(t) = Asin(at^2) \tag{3.8}$$

where A is amplitude the chirp signal.

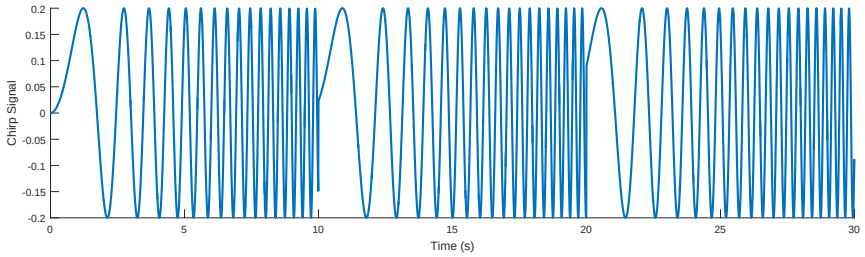

Figure 3.1: Chirp signal to be used excite the system for system identification

As given in Section 3.1, we can obtain extended power spectral density, $S_{UU}(\omega)$, and extended cross spectral density, $S_{UY}(\omega)$ of LTP systems by using input and

output pairs. However, they are different from the spectral density functions of LTI system due to matrix properties. Spectral density functions of LTP system can be defined as follows:

$$\begin{aligned} S_{UU} &= U^{*T}U \\ S_{UY} &= U^{*T}Y \end{aligned} \tag{3.9}$$

Then, we can write the following equality which expresses the estimated harmonic transfer functions of LTP system as follows:

$$\hat{H}(\omega) := \begin{bmatrix} \hat{H}_1 \\ \hat{H}_0 \\ \hat{H}_{-1} \end{bmatrix} = (S_{UU})^{-1}S_{UY} \tag{3.10}$$

which is analogous to transfer function expression of LTI system in (3.6).

After we obtain the extended spectral density functions, we have same relation with estimation of transfer function of LTI systems. However, such a calculation for estimation of HTFs cannot provide accurate results since we truncate the number of harmonics beyond a certain order which may cause an error. Therefore, in order to increase prediction performance of harmonic transfer functions, [6] adds an unmodeled part as an error, $E(j\omega)$, to the output response which can be expressed as

$$\begin{aligned} Y(j\omega) &= \sum_{n=-1}^{1} U(j\omega - nj\omega_0)\hat{H}_n + E(j\omega) \\ &= U^T\hat{H} + E(j\omega) \\ &= \hat{Y}(j\omega) + E(j\omega), \end{aligned} \tag{3.11}$$

where Y and $\hat{Y}$ represents measured and estimated outputs respectively.

Here, the error expresses difference between the predicted hramonic transfer functions and measured system response. Then, [6] defines a cost function in order to reduce error term and formulate the problem as a minimization of a cost function, J, which penalizes the curvature of HTFs and quadratic error which is given as,

$$J = min_{\hat{H}}[(Y - U^T\hat{H})^2 + \alpha(D^2\hat{H})^2] \tag{3.12}$$

Here α is a constant and D^2 represents second order differential operator in order to tune smoothness of predicted transfer functions. Then, we take the derivative of the cost function, J, with respect to $\hat{H}$ in (3.12), and we find the minimizing $\hat{H}$ as:

$$\hat{H}(j\omega) = (S_{UU} + \alpha D^4)^{-1} S_{UY}. \tag{3.13}$$

The results of equation (3.13) provides a formula to identify harmonic transfer function of LTP system via input-output pairs.

3.2.2 System Identification with Single Cosine Input Signal

The goal of this section is to develop a procedure in order to predict harmonic transfer function of LTP systems. In order to achieve this goal successfully, excitation input signal plays a crucial role. In Section 3.2.1, we illustrate the frequency domain system identification methodology of [6] by using chirp excitation signals. Among various types of excitation signals the frequency sweep input is a favorable choice for frequency domain identification. However, there is a problem in using the chirp signal as an excitation input signal since if one excite the LTP system at its fundamental frequency, ω_0, the output response generates incorrect signals around pumping frequency of the system. In order to avoid this problem, the input signal should not include a component at pumping frequency but chirp input signal does not satisfy this requirement. In Section 2.3.1, the test signal is exponentially modulated periodic signal and spectral functions are obtained via modulated complex Fourier series expansion of EMP signals. From this point of view, in [5] , a different excitation input signal by using complex exponentially modulated periodic signal to describe transfer functions of LTP system is developed. To create a complex exponentially modulated periodic signal at frequency, ω_f, sine and cosine signals can be summed as follows:

$$\begin{aligned} u(j\omega_f, t) &= |u| \, (cos\omega_f t + j sin\omega_f t) \\ &= |u| \, e^{j\omega_f t} \end{aligned} \tag{3.14}$$

Another approach to excite LTP systems is to use single sine or cosine input signal at a specific frequency, ω_f. Since this type of excitation input signals are generally used to identify LTI system, it can be adopted to identify LTP systems easily. The excitation of an LTI system with a single cosine input is shown in the diagram given by Fig. 3.2.

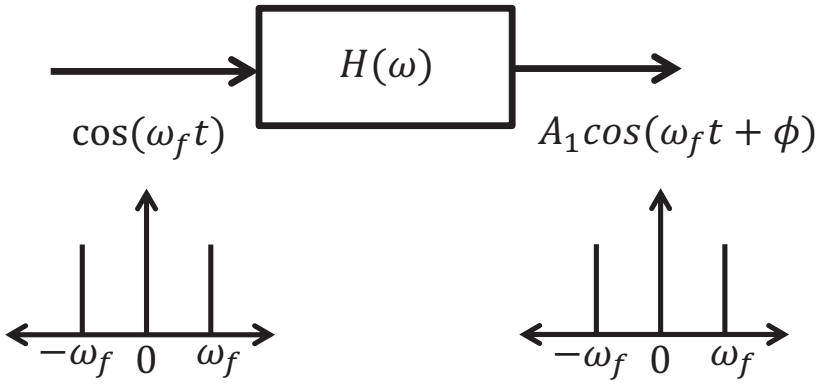

Figure 3.2: Input-output relation of LTI systems when single cosine signal is applied

According to this diagram, if we apply cosine signal at a specific frequency, ω_f, the system generates an output at that frequency with different magnitude and phase. Transfer function identification of LTI system is achieved by following computation.

$$\hat{H}(\omega_f) = \frac{U^*(\omega_f)Y(\omega_f)}{U^*(\omega_f)U(\omega_f)} \tag{3.15}$$

In order to complete identification of LTI systems, the test procedure should continue until desired frequency range is swept.

LTP systems differ from LTI systems regarding output response since if one apply cosine signal input with a specific frequency to the LTP system, output includes multiple harmonics with different magnitudes and phases at harmonic frequencies of fundamental frequency within itself. The example diagram of input output relation of LTP system with single cosine input signal is illustrated in Fig. 3.3.

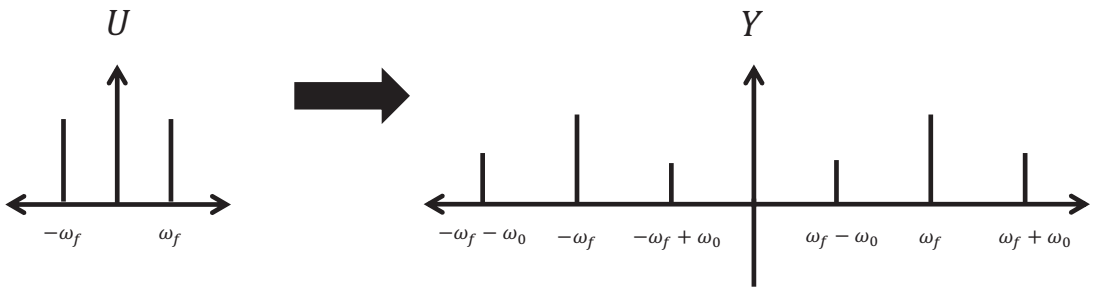

Figure 3.3: Input-output relation of LTP systems when single cosine signal is applied

Harmonic transfer function identification of this system is given in following equation.

$$\hat{H}_{\mp n}(\omega_f \mp n\omega_0) = \frac{U^*(\omega_f)Y(\omega_f \mp n\omega_0)}{U^*(\omega_f)U(\omega_f)} \tag{3.16}$$

where U and Y represent Fourier transform of input, $u(t)$ and output, $y(t)$. Input and output of LTP system can be defined as follows in time domain:
Input: $u(t) = cos(\omega_f t)$
Output: $y(t) = \sum_{n=-M}^{M} A_n cos((\omega_f + n\omega_0)t + \phi_n)$
Here, M corresponds to the number of harmonics and $A_n = A_{-n}^*$ and ϕ_n belongs to the phase of nth harmonic.

In order to complete system identification of LTP systems via this way, identification process defined in (3.16) should be repeated for different values of specific frequency, ω_f. After finishing all test process, one can obtain the following structure of estimated HTFs.

$$\hat{\mathcal{H}}(s) = \begin{bmatrix} \ddots & \vdots & \vdots & \vdots & \\ \dots & \hat{H}_0(s-j\omega_0) & \hat{H}_{-1}(s) & \hat{H}_{-2}(s+j\omega_0) & \dots \\ \dots & \hat{H}_1(s-j\omega_0) & \hat{H}_0(s) & \hat{H}_{-1}(s+j\omega_0) & \dots \\ \dots & \hat{H}_2(s-j\omega_0) & \hat{H}_1(s) & \hat{H}_0(s+j\omega_0) & \dots \\ & \vdots & \vdots & \vdots & \ddots \end{bmatrix}. \tag{3.17}$$

3.2.3 System Identification with Sum of Cosine Input Signal

In previous section, we examined system identification of LTP systems via single cosine input signal. As exciting the system with single cosine signal with a specific frequency creates an output which is the superposition of cosine signals at different frequencies with diverse magnitudes and phases. By using (3.16), one can obtain the estimated harmonic transfer function at that excitation frequency of the input. However, using single cosine input signal requires multiple experiments in order to cover the frequency range which we are interested in our study. In order to handle this problem, summation of cosine input can be used rather than single cosine signal which is proposed by [44, 45]. Since the output of single cosine signal at a specific frequency consists of multiple harmonics, in order to use sum of cosine signals as an input, it should be guaranteed that the harmonics of the different frequency cosine signals do not coincide. Hence, the main objective of this section is to compose a formula for input signal which consists of sum of different cosine signals where their outputs do not coincide. Before we give the formula for sum of cosine signal, first define certain terms which will be used in the sequel.

Table 3.1: Table of Definition in the Formula of Sum of Cosine

f_0	$\triangleq$	Fundamental frequency of LTP system
f_r	$\triangleq$	Frequency resolution in frequency domain
f_{dr}	$\triangleq$	Desired frequency resolution in input signal.
f_{max}	$\triangleq$	Maximum value of frequency range of input signal.
N_{st}	$\triangleq$	Number of frequency contained in a test
N_{fb}	$\triangleq$	Number of band
N_{bt}	$\triangleq$	Number of tests that can be performed in a band

Formulas for some definitions

$$N_{st} = \frac{f_0}{2f_{dr}}$$
$$N_{fb} = \frac{f_{max}}{f_0}$$
$$N_{bt} = \frac{N_{st}}{N_{fb}}$$

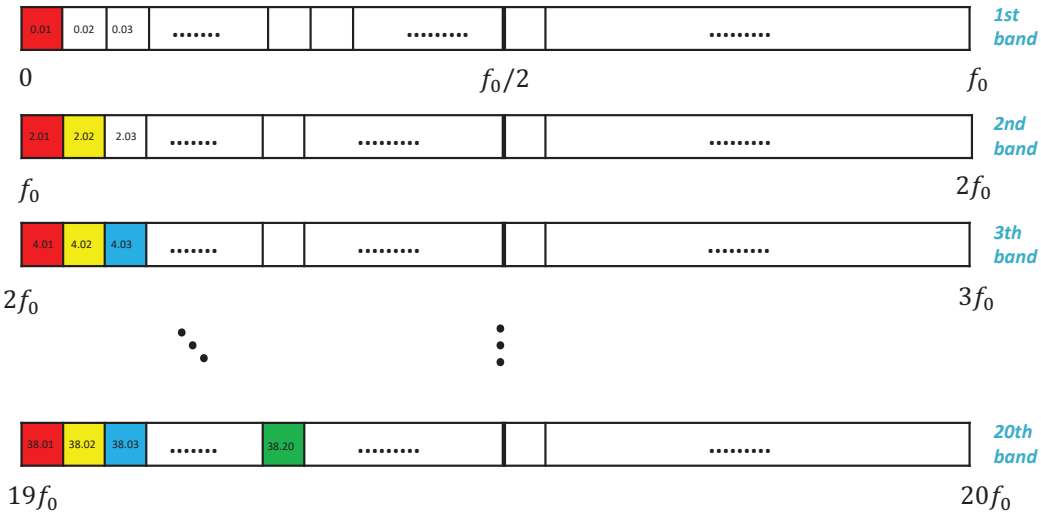

Figure 3.4: Locations of the frequencies included in Sum of Cosine input signal. Sum of cosine input signal includes only one of the frequencies which are same color.

In Table 3.1, definitions of some terms used in the sum of cosine and formulas for some of the terms are given. The first rule for the sum of cosine input signal is

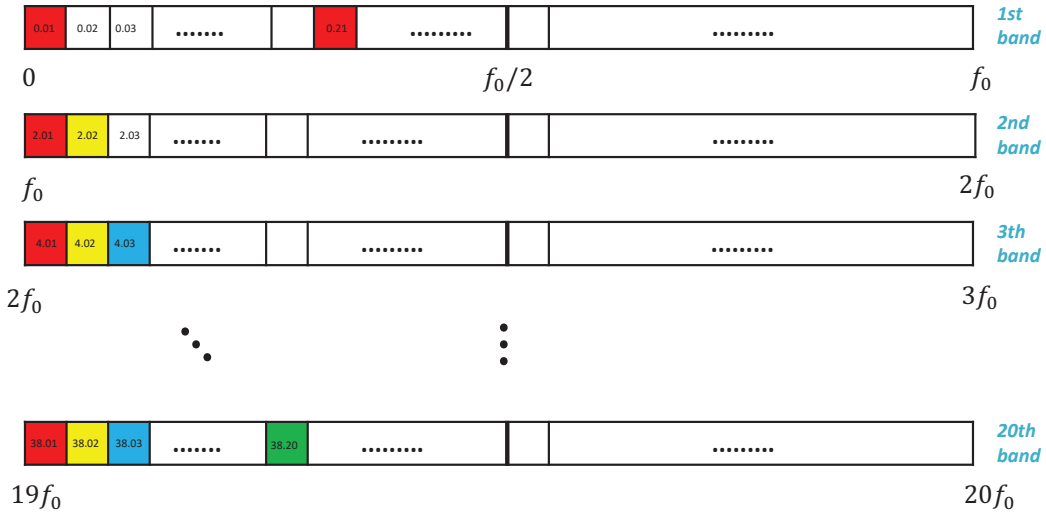

Figure 3.5: Locations of the frequencies included in Sum of Cosine input signal.

that the harmonics of the output of separated cosine signals should not coincide. Since every cosine signal with a frequency, ω, produces an output at frequencies $\omega \mp n\omega_0$. In order to prevent this issue, we first separate the frequency range that we are interested in the study as the frequency bands. The length of one frequency band should be equal to pumping frequency, f_0, of LTP system. Thus, number of frequency bands required is obtained by division of maximum value of frequency range, f_{max}, of input with the pumping frequency, f_0. For the sake of clarity, proposed procedure is illustrated in Fig. 3.4. In Fig. 3.4, sum of cosine input signal should contain only one of the frequencies which are of the same color. The reason behind of this is to prevent coincide issue of the harmonics of the input frequencies. For instance; when the sum of cosine signal includes a cosine signal with frequency $f_1 = 0.01$, the LTP system will produce an output at frequencies $f_1 \pm nf_0$ where $n \in Z$. So, if the sum of cosine input also include cosine signal at the frequency $f_2 = f_1 + f_0$, its corresponding output also produces harmonics at frequencies $f_2 \pm nf_0$. That is, the outputs of these cosine input signals will coincide. Therefore, in order to avoid this issue, the input frequencies of these signals should not be in the locations which are illustrated with same color in Fig. 3.4. In Fig. 3.5, different from Fig. 3.4 there is a new red box with frequencies $f = 0.21$. The first sliding frequency process is completed and the new sliding frequency for the input frequencies of sum of cosine input signals is

started. This process is continued to until first half of the first band is ended up. In the light of these information, sum of cosine input signal formula is developed for the first and second halves of the frequency bands in equation (3.18).

$$\begin{aligned} u(t) &= \sum_{l=1}^{N_{fb}} \sum_{k=0}^{N_{bt}-1} cos(2\pi(f_r + (l-1) \times (f_p + f_{dr}) + N_{fb} f_{dr} k)t), \\ u(t) &= \sum_{l=1}^{N_{fb}} \sum_{k=0}^{N_{bt}-1} cos(2\pi(f_r + (l-1) \times (f_p + f_{dr}) + N_{fb} f_{dr} k + \frac{f_0}{2})t). \end{aligned} \tag{3.18}$$

3.3 Application Example: Simplified Legged Locomotion Models

In this section, we use a simple, vertically constrained spring–mass–damper system model as our test example. Actually, in the literature there are more general legged locomotion models, which can represent planar legged robot platforms with a high accuracy [46]. However, we constrain our model to a vertical motion only to ensure analytical derivation of harmonic transfer functions as a ground truth for our data-driven system identification methodology. Such simplified models has also been used in the literature to evaluate the prediction performance of HTFs for legged locomotor systems [41] even in the presence of input and measurement noise [47] using chirp input excitations. Different than these works, we aim to increase system identification performance using sum of cosine inputs. We also provide comparative results to demonstrate the efficiency of proposed system identification strategy.

3.3.1 System Dynamics of Simplified Legged Locomotion Model

Simplified vertical leg model is illustrated in Fig. 3.6. This system includes a mass connected to a leg and spring mass damper mechanism with force transducer. There are two phases which are stance and flight phase where damper is turned

off and that behavior provides periodicity for this system. Force transducer is used both for energy supply and system identification purposes. In [8], there is also a similar model but it uses additional nonlinear spring differently from this system.

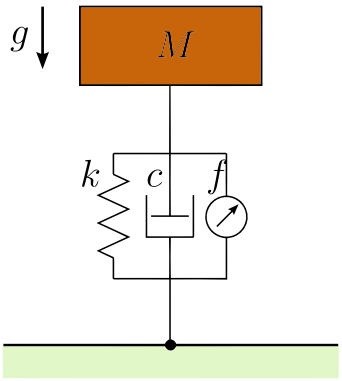

Figure 3.6: Simplified leg model with spring mass damper system including linear force transducer.

Equations of motion of simplified legged model are presented in [41] as:

$$m\ddot{x} = \begin{cases} -mg - c\dot{x} - k(x - x_0) + f(t), & \text{if } \dot{x} > 0 \\ -mg - k(x - x_0) + f(t), & \text{otherwise} \end{cases} \tag{3.19}$$

where $f(t)$ is an external force. Parameters of this system are chosen as $k = 200$, $g = 9.81$, $c = 2$, $x_0 = 0.2$ and $m = 1$ in [48]. Linear actuator input is $f(t) = f_0(t) + u(t)$ where $f_0(t)$ is used to compensate energy losses and $u(t)$ is used to perturb the system for system identification purpose.

3.3.2 Theoretical Computation of HTFs of Simplified Legged Locomotion Model

In this section, we aim to obtain harmonic transfer functions of spring mass damper model around its limit cycle. To accomplish this, we first acquire system dynamics of error trajectories which is computed by subtracting output response

of this system from the measured limit cycle. In order to induce the system to a stable limit cycle, in [41] $f_0(t)$ is chosen as $cos(2\pi t)$. Here, $\bar{x}(t)$ represents the state vector in limit cycle. By choosing error vector as $\xi(t) = x(t) - \bar{x}(t)$ and by substituting it into the equation of motion in above, we obtain:

$$\ddot{\xi}(t) = \begin{cases} -k\xi - c\dot{\xi}, & \text{if } \dot{\xi} + \dot{\bar{x}}(t) > 0 \\ -k\xi, & \text{otherwise} \end{cases} \tag{3.20}$$

Then, we obtain state space representation of equation (3.20) as,

$$\begin{aligned} \begin{bmatrix} \dot{\xi}_1 \\ \dot{\xi}_2 \end{bmatrix} &= \begin{bmatrix} 0, 1 \\ -k - cr(t) \end{bmatrix} \begin{bmatrix} \xi_1 \\ \xi_2 \end{bmatrix} + \begin{bmatrix} 0 \\ 1 \end{bmatrix} u(t), \\ y &= \begin{bmatrix} 1, 0 \end{bmatrix} \begin{bmatrix} \xi_1 \\ \xi_2 \end{bmatrix}. \end{aligned} \tag{3.21}$$

where $\dot{\xi}_1 = \xi_2$ and $\dot{\xi}_2 := \ddot{\xi}_1 = \ddot{\xi}$. Also, $r(t) = 1$, if $\dot{\xi} + \dot{\bar{x}}(t) > 0$ and $r(t) = 0$ otherwise which provides periodicity. Now, we obtain the state space representation of error around limit cycle of legged model. Placing these matrices into the theoretical computation part as given in Section 2.3, we can obtain the analytical solution of harmonic transfer functions of this model. We use the results of theoretical computation of HTFs in order to compare prediction performance of system identification methods in the sequel.

Estimation of HTFs of Legged Model via Chirp Input Signal

In this section, we aim to predict harmonic transfer function of linearized dynamics of legged model presented in (3.21). An important point is we do not have any knowledge about state space dynamics of the model and only use input output data to estimate HTFs. We first need to measure limit cycle data during 30 cycles without perturbing the system and choose $f_0(t) = cos(2\pi t)$ and $u(t) = 0$. Then, in order to perturb the system, input signal is computed by using *chirp* command of $Matlab$ environment. The magnitude of this input chirp signal, $u(t)$, is chosen as 0.001 with linearly increasing frequency range between $(0, 20]\ Hz$. After that

output of the system is subtracted from the measured limit cycle data and we obtain error data, ξ_1. By using input chirp signal, $u(t)$, and error trajectory, ξ_1, we obtain harmonic transfer function of the system by using the methodology represented in [6, 41] through the equation from (3.8) to (3.13). Estimation results will be given after explaining the all system identification techniques in Section 3.2.1, Section 3.2.2 and Section 3.2.3.

Estimation of HTFs of Legged Model via Single Cosine Input Signal

Differently from previous section, here we perturb the system by using single cosine signal with magnitude of 10^{-4}. That is, the input signal is determined as $u(t) = 10^{-4}cos(2\pi f_c t)$ where desired frequency range to be recovered, $f_c \in (0, 20]Hz$ with 0.01 Hz resolution. In order to recover desired frequency range, we make 2000 different experiment with single cosine input signals.

Estimation of HTFs of Legged Model via Sum of Cosine Input Signal

In this section, we repeat same identification method of single cosine signal input by using the formula of sum of cosine signal we developed. The terms in Table 3.1 is determined as following:

f_0	f_r	f_{dr}	N_{st} $(\frac{f_0}{2f_{dr}})$	N_{fb} $(\frac{f_{max}}{f_0})$	N_{bt} $(\frac{N_{st}}{N_{fb}})$
2	0.01	0.01	100	20	5

Table 3.2: Values of Parameters in Sum of Cosine Formula

Number of frequency included in sum of cosine input signal, N_{st}, is equal to 100. That is, we can recover 100 different frequencies in one test. Total number of frequencies should be recovered is equal to 2000. Hence, we can recover all frequencies and complete estimation of harmonic transfer functions with 20 tests and decrease the number of required tests by 100 times.

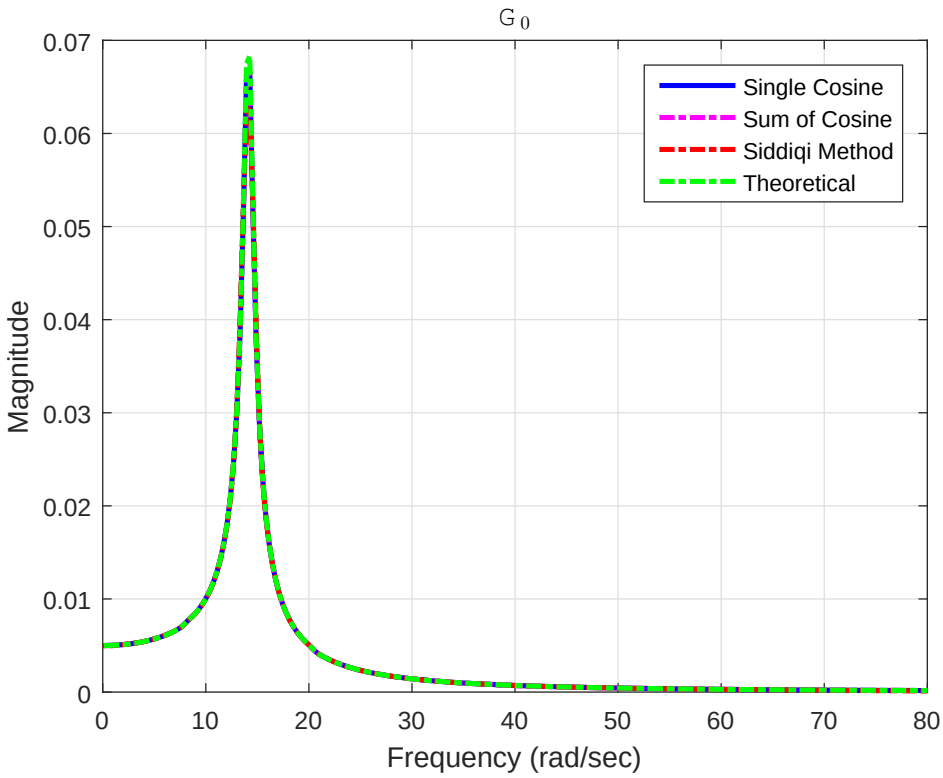

Figure 3.7: Prediction results of fundamental harmonic transfer functions.

Now, we will show the estimation performances of three different system identification methods with theoretical computation of harmonic transfer function of this model. Fig. 3.7 shows the estimation performance of proposed system identification methods with respect to theoretical derivation of fundamental harmonic transfer function. As red dot-line corresponds to prediction result of Siddiqi's identification method with chirp input signal, blue line and magenta dot-line show estimation results of identification methods with single cosine and sum of cosine input signal respectively. The graph illustrates that all of the methods works well to estimate HTFs of simple legged model. It is also valid for the estimation of first harmonics. However, for higher harmonics such as second and third, it is seen that Siddiqi's method could not estimate HTFs in some regions, especially G_2 and G_{-2}. Fortunately, the estimation performance of single sine and sum of cosine signal inputs seem to work well even in the some frequency regions where Siddiqi's method could not correctly predict HTFs. The estimation results are shown in Fig. 3.8, Fig. 3.9 and Fig. 3.10.

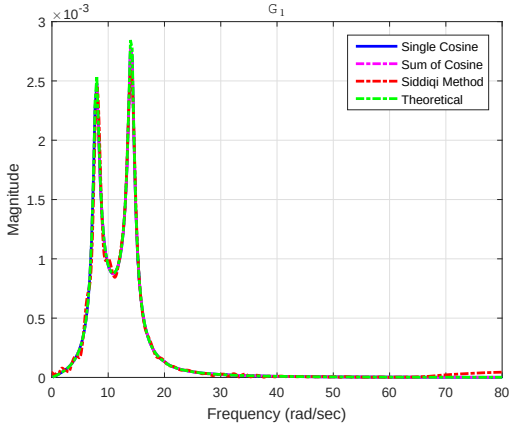

(a) G_1

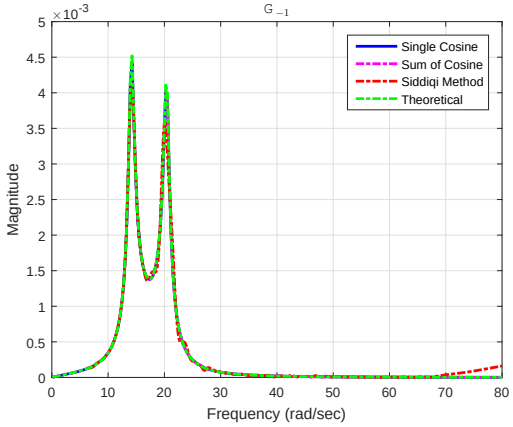

(b) G_{-1}

Figure 3.8: Prediction results for the higher order harmonics. The magnitude plots of the first harmonics are represented as a comparison of theoretical computation and data driven identification methods with chirp, single cosine and sum of cosine input signals.

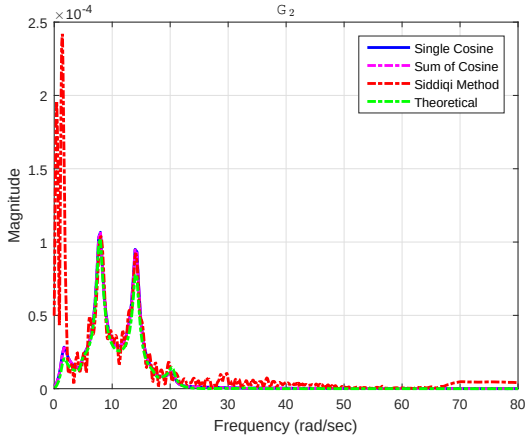

(a) G_2

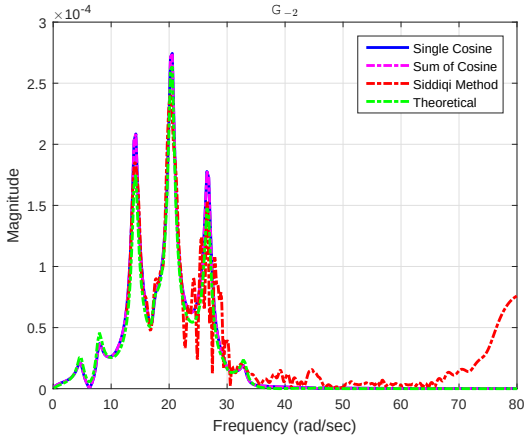

(b) G_{-2}

Figure 3.9: Prediction results for the higher order harmonics. The magnitude plots of the second harmonics are represented as a comparison of theoretical computation and data driven identification methods with chirp, single cosine and sum of cosine input signals.

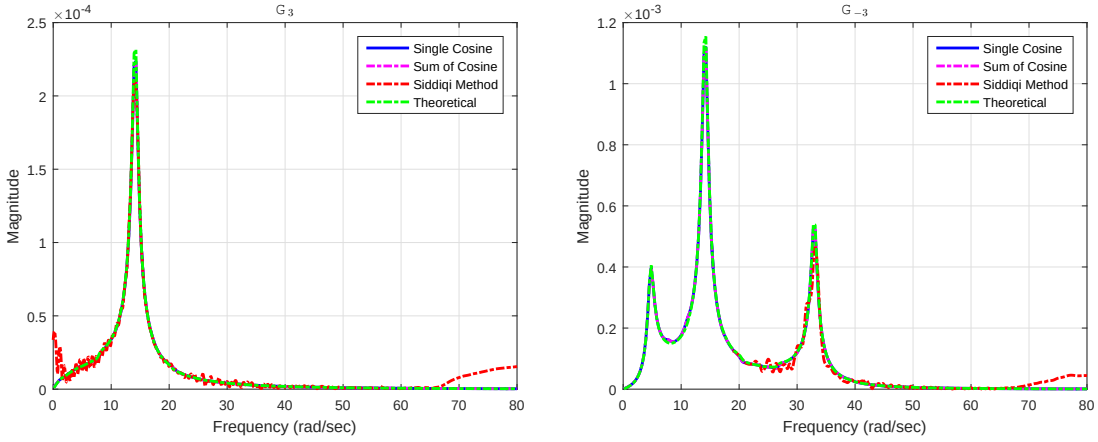

(a) G_3 (b) G_{-3}

Figure 3.10: Prediction results for the higher order harmonics. The magnitude plots of the third harmonics are represented as a comparison of theoretical computation and data driven identification methods with chirp, single cosine and sum of cosine input signals.

As a result, we illustrate the prediction performance of estimated harmonic transfer functions via three different data driven identification methods. In some frequency regions, identification results of chirp input signal provides incorrect results. Fortunately, single cosine input signal can predict the HTFs even in these regions. However, this method requires multiple experiments in order to recover desired frequency range. The sum of cosine input signal provides successful prediction performance beside decrease the computational time by $f_0/2f_{dr}$ times where f_0 is pumping frequency and f_{dr} is the desired frequency resolution.

Chapter 4

Stability Analysis and Control of LTP Systems via Nyquist Criterion with HTFs

The goal of this chapter is to investigate the stability characteristics of LTP systems and design controllers to increase stability and/or enhance performance. The stability of LTI systems can be simply analyzed via the well-known Nyquist stability test. This chapter focuses on how the Nyquist stability test can be applied to understand stability characteristics of LTP systems. The main idea here is that LTP systems can be represented with equivalent MIMO LTI systems, hence we should be able to use Nyquist test for stability analysis of LTP systems as well. Nyquist diagram of linear time periodic system is constructed via eigenloci of harmonic transfer functions. In this chapter, Nyquist criterion is used for two purposes which are to determine closed loop stability of LTP systems and in order to design P, PD and PID controllers to stabilize and enhance system performance of LTP systems based on Nyquist graphs. In this respect we first show the construction of Nyquist diagram of linear time periodic systems via eigenloci of theoretical harmonic transfer functions and usability of Nyquist stability criterion in order to assess the stability characteristics of these systems. Then, we illustrate how to obtain Nyquist diagram of LTP systems by using input-output

data without having any knowledge about state space model the system. After giving some preliminary knowledge about HTF representation of LTI controller, we design P, PD and PID controllers based on Nyquist diagrams.

4.1 Stability Analysis of LTP Systems via Nyquist Criterion with Theoretical HTFs

One of the pioneering and most significant studies on the stability analysis of periodic systems is the Floquet theory [24, 49], especially for examining stability of rotating machinery such that wind turbines [3, 50], helicopter rotors [4, 37, 51], and so on. Stability analysis of linear time periodic systems also can be achieved via Lyapunov theory [25] or Hill determinant technique [26]. However, these techniques answer the stability question of LTP systems for only a specific value of gain. However, the ability to identify feedback gain ranges that can stabilize a periodic system and to use these values that optimize system performance among them in controller design will undoubtedly make a significant contribution to the control of periodic systems. As a result of this motivation, stability analysis of LTP systems via Nyquist criterion provides closed loop stability for a function of feedback gain. In control theory, classical Nyquist stability criterion is developed for Single Input Single Output (SISO) systems [52]. Then, this notation is extended to the Multi Input Multi Output (MIMO) systems in different ways [53, 54]. Finally, MIMO Nyquist stability criterion which depends on eigenloci of transfer function matrix is developed by [55].

Since as seen from Section 2.3.3, LTP systems can be treated as a LTI system with infinitely multi inputs and multi outputs [9], a Nyquist criterion for LTP system based on Nyquist criterion of MIMO systems is presented in [20]. Thus, when feedback is applied, instead of deciding closed loop stability of LTP system for a single value of feedback gain, plotting eigenloci of LTP harmonic transfer function provides determination of stability for a family of gain parameters. In this part, we illustrate how to apply Nyquist criterion in order to analyze stability

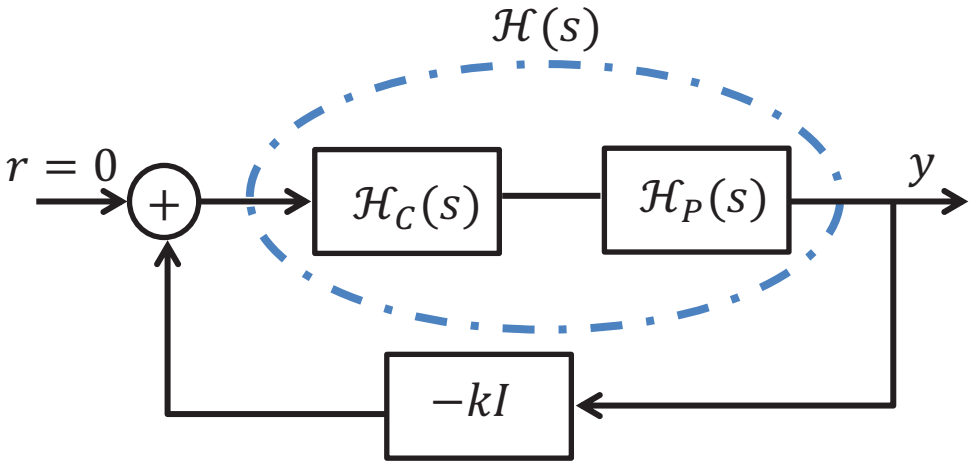

Figure 4.1: Closed Loop Feedback System.

of the closed loop system illustrated in Fig. 4.1. In LTI system, closed loop stability analysis with feedback gain k can be examined by plotting Nyquist contour of transfer function $H_0(j\omega)$ for frequency range $-\infty < \omega < \infty$ and counting encirclements of the point $-1/k$. In LTP systems, in order to obtain eigenloci of harmonic transfer functions, it is proposed in [20] that using standard eigenvalue computations of HTFs produces number of closed curves and stability can be determined by counting encirclements of the point $-1/k$ which is given in following Theorem 4.1.1.

Theorem 4.1.1. *[20] Assume that there is a linear, periodic input output relation from r to y shown in Fig. 4.1. Denote the eigenvalues of the doubly infinite Toeplitz form matrix $\mathcal{H}(s)$ given in (4.1) for s varying through the dotted contour in Fig. 4.2, which is denoted as the fundamental strip as $\{\lambda_i(s)\}_{i=-\infty}^{\infty}$. These eigenvalues generate a number of closed curves in the complex plane which is called as eigenloci of the harmonic transfer functions. The feedback system illustrated in Fig. 4.1 is stable from input, r, to the output, y if and only if the total number of counterclockwise encirclements of the point $-1/k$ of these closed curves equals to the number of right half plane poles of open loop harmonic transfer function, $\mathcal{H}(s)$ in the fundamental strip.* □

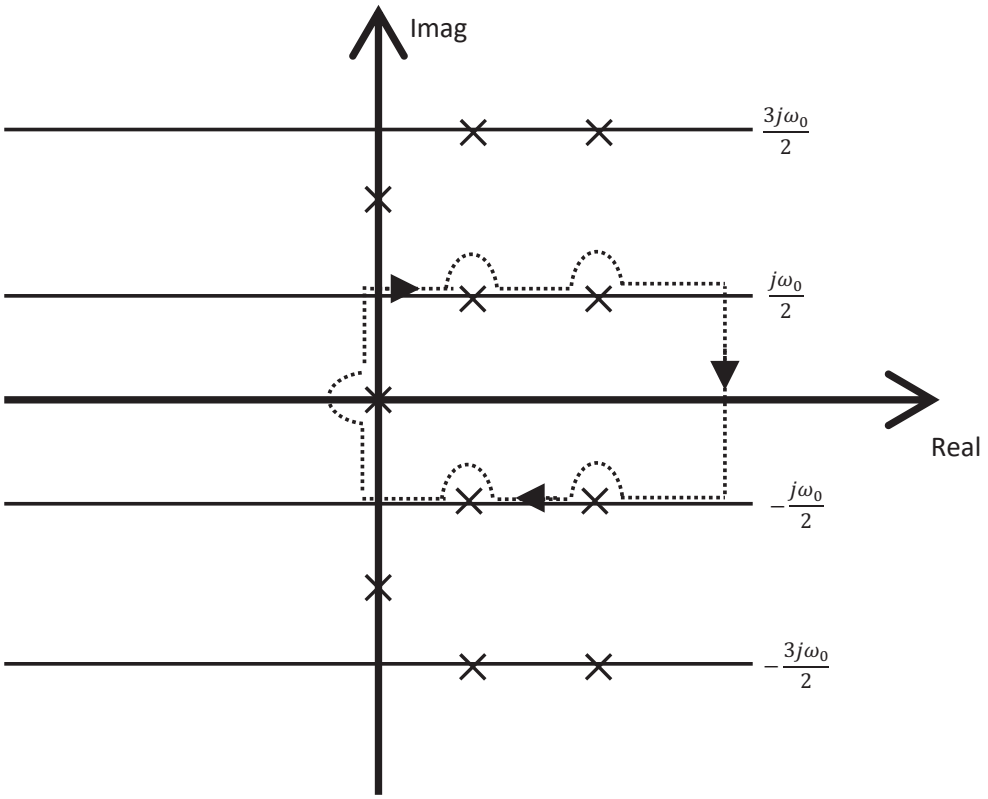

Figure 4.2: The contour for Nyquist Criterion with Harmonic Transfer Functions in s Plane which is denoted by $\bar{N}_f$. The notation "$\times$" corresponds to the poles of $\mathcal{H}(s)$.

$$\mathcal{H}(s) = \begin{bmatrix} \ddots & \vdots & \vdots & \vdots & \\ \dots & H_0(s-j\omega_0) & H_{-1}(s) & H_{-2}(s+j\omega_0) & \dots \\ \dots & H_1(s-j\omega_0) & H_0(s) & H_{-1}(s+j\omega_0) & \dots \\ \dots & H_2(s-j\omega_0) & H_1(s) & H_0(s+j\omega_0) & \dots \\ & \vdots & \vdots & \vdots & \ddots \end{bmatrix}. \tag{4.1}$$

In [13], eigenloci of HTFs is parametrized by $s \in \bar{N}_f$ and Hill determinant is

expressed as $\left|I + k\mathcal{H}(s)\right|$ regarding eigenvalues of HTFs as

$$\left|I + k\mathcal{H}(s)\right| = \prod_{n=-\infty}^{\infty} (1 + k\lambda_n(s)). \tag{4.2}$$

Here, the product formulation is infinite due to the doubly infinite transfer function $\mathcal{H}(s)$. In order to implement this formula on computer, it has to be truncated, so, we separate the equation (4.2) into the two parts as following:

$$\left|I + k\mathcal{H}(s)\right| = \prod_{n=-M}^{M} (1 + k\lambda_n(s)) \prod_{n\notin[-M,M]} (1 + k\lambda_n(s)) \tag{4.3}$$

The first M harmonics of the HTFs can be treated as significant parts and others cannot be considered as necessary since they do not contribute to the encirclement of the point $-1/k$. This is because, the eigenvalues which indices greater than M remain inside the unit disk, D_c. So, number of eigenvalues of first M harmonic transfer function given in (4.3) can be counted as encirclements. As a result, eigenloci of truncated harmonic transfer functions are obtained by computing eigenvalues of these HTFs through the Nyquist path, $\bar{N}_f$ illustrated in Fig. 4.2 and plotted to the complex plane. The closed loop stability of the system is provided if and only if the point, $-1/k$ is encircled counterclockwise direction n_p times which is equal to the number of right half plane poles of truncated HTFs in fundamental strip.

Poles of LTP Systems in s plane

The places where the harmonic transfer function is not analytical give the poles of the LTP systems in the complex plane. As it is seen in equation (4.1), the poles of the system consists of the poles of LTI transfer functions, $H_k(s)$. In complex s plane, the solution of following eigenvalue problem gives the poles of LTP system,

$$\left\{s\mathcal{I} - (\mathcal{A} - \mathcal{N})\right\}\mathcal{V} = 0. \tag{4.4}$$

The solution gives infinite poles however, in order to obtain the right half plane poles of the LTP systems figured in Theorem 4.1.1 we look at the poles which are placed in fundamental strip whose range given by,

$$Im(s) \in (-\frac{\omega_0}{2}, \frac{\omega_0}{2}].$$

4.1.1 Wereley Example: Stability Analysis of Mathieu Equation

In this section, we aim to illustrate numerical example for closed loop stability analysis of Mathieu equation's parameters by using Nyquist criterion. In order to achieve that, we use the example given in [13]. Stability of Mathieu example was investigated in many different studies [56–58]. Equation of lossy Mathieu equation is given by,

$$\ddot{x}(t) + 2\zeta\dot{x}(t) + (a - 2qcos(\omega_0 t))x(t) = 0 \tag{4.5}$$

The fundamental frequency of this equation is given as $\omega_0 = \pi$ in [13]. State variables of the Mathieu equation defined as:

$$\begin{aligned} x_1(t) &:= x(t) \\ x_2(t) &:= \dot{x}_1(t) = \dot{x}(t) \\ \dot{x}_2(t) &:= \ddot{x}_1(t) = \ddot{x}(t) \end{aligned} \tag{4.6}$$

Using these state variables, (4.6), in equation (4.5) gives the following state space model:

$$\begin{aligned} \dot{x}(t) &= A(t)x(t) + B(t)u(t) \\ y(t) &= C(t)x(t) + D(t)u(t) \end{aligned} \tag{4.7}$$

where

$$\begin{aligned} A(t) &= \begin{bmatrix} 0 & 1 \\ -(a - 2qcos\omega_0 t) & -2\zeta \end{bmatrix}, \\ B &= \begin{bmatrix} 0 \\ 1 \end{bmatrix} \quad C = \begin{bmatrix} 1 & 0 \end{bmatrix}, \\ D &= \begin{bmatrix} 0 \end{bmatrix}. \end{aligned} \tag{4.8}$$

Examining stability of the Mathieu equation with respect to system parameters, (q, a) is achieved by Floquet theory in [13]. Therefore, to analyze stability of Mathieu equation we first compute the fundamental monodromy matrix, $\phi(T, 0)$,

of the system shown in (4.8) for each (q, a) pair by solving following first order differential equation and and obtaining the value of $\Phi(t, 0)$ at time T:

$$\dot{\Phi} = A\Phi. \tag{4.9}$$

Here, we solve the equation (4.9) by using *ode*45 function of *Matlab* which integrates the system of differential equations. At each point of (q, a), we solve the differential equation and compute the monodromy matrix, $\Phi(T, 0)$. If the maximum absolute value of eigenvalue of $\Phi(T, 0)$ is inside the unit disc, that is less than 1, the system is saved as stable for this value of (q, a) pair. According to the results of this stability test, following graph is obtained with respect to value of (q, a). Fig. 4.3 illustrates stable and unstable regions of lossy Mathieu

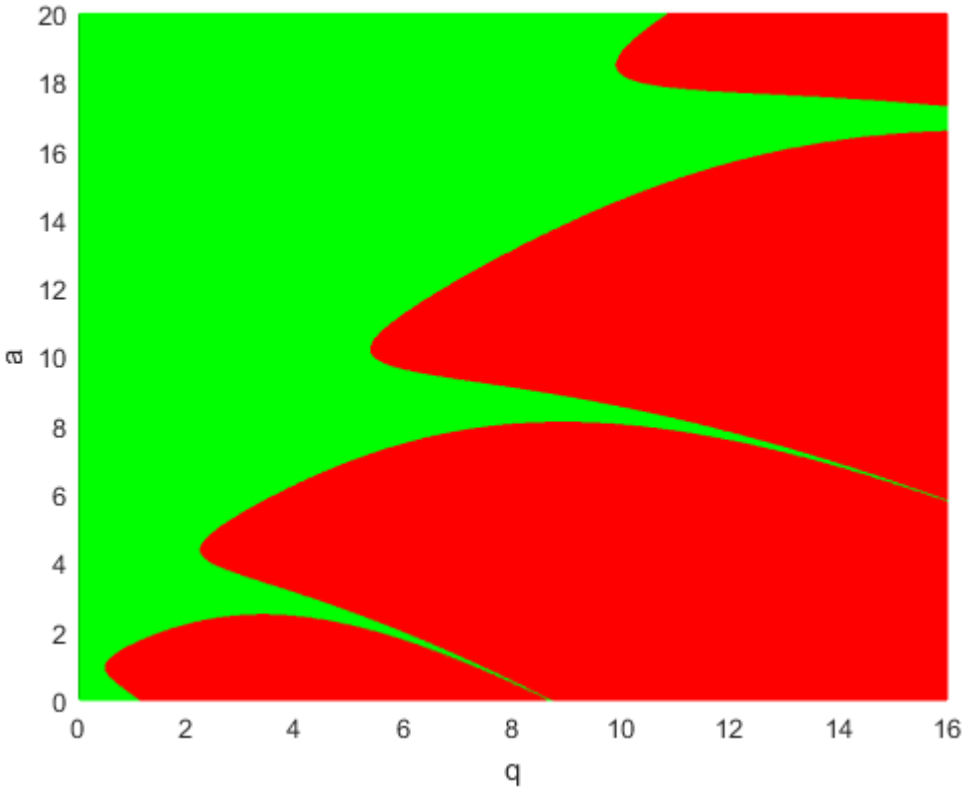

Figure 4.3: Stability analysis of lossy Mathieu equation with respect to (q, a) by using Floquet theory. As red regions corresponds to the value of (q, a) which makes system unstable, green regions belong to the stable regions.

equation with respect to the value of (q, a). In order to obtain this graph, first

order differential equation is solved and maximum absolute value of eigenvalues of this equation is investigated for each value of (q, a) which was the disadvantage of Floquet theory. Here, in order to show advantage of Nyquist stability test, Wereley illustrate the application of Nyquist criterion on this example in the following.

Stability Analysis with Nyquist Criterion

In order to apply Nyquist criterion on lossy Mathieu equation, a new parameter $\beta = q/a$ is defined in [13] and equation (4.5) can be written as

$$\ddot{x}(t) + 2\zeta\dot{x}(t) + a[1 - 2\beta cos(\omega_0 t)]x(t) = 0 \tag{4.10}$$

β is related with the periodic effects on this example such that if $\beta \ll 1$, system does not behave as time periodic but for the larger values of β, periodicity of the system will increase. If we design system parameter as feedback gain, we can apply Nyquist criterion in order to analyze stability of the system in terms of variations of q and a. As a result of this motivation, feedback control law is defined in [13] as,

$$u(t) = -ax(t) \tag{4.11}$$

Substituting equation (4.11) into the equation (4.10) gives:

$$\ddot{x}(t) + 2\zeta\dot{x}(t) + [1 - 2\beta cos(\omega_0 t)]u(t) = 0 \tag{4.12}$$

In [13], the modified equation (4.10) is represented as in the Fig. 4.4. In this figure, LTI transfer function, $H_p(s)$ is:

$$H_p(s) = \frac{1}{s(s + 2\zeta)} \tag{4.13}$$

In Fig. 4.4, a parameter can be examined as feedback gain k. System matrices after modification of state space model in (4.7) are given as following,

$$A(t) = \begin{bmatrix} 0 & 1 \\ 0 & -2\zeta \end{bmatrix},$$

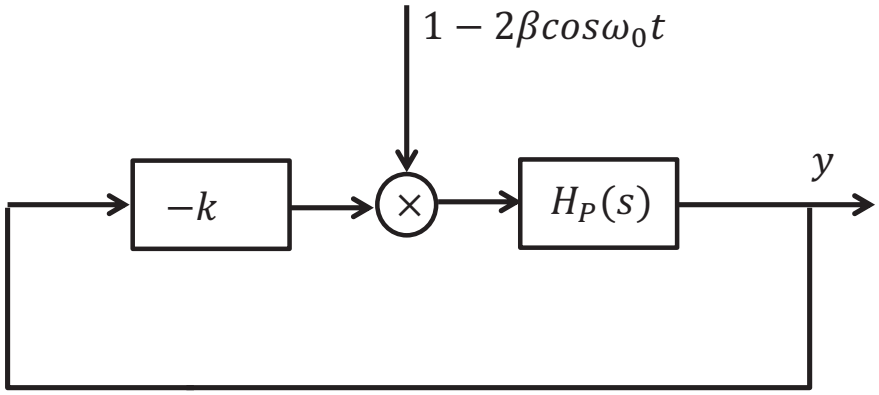

Figure 4.4: Block diagram of lossy Mathieu equation with feedback gain law. Input of the LTI transfer function, $H_p(s)$, is modulated with time periodic signal.

$$B = \begin{bmatrix} 0 \\ (1 - 2\beta cos\omega_0 t) \end{bmatrix} \quad C = \begin{bmatrix} 1 & 0 \end{bmatrix}, \tag{4.14}$$
$$D = \begin{bmatrix} 0 \end{bmatrix}.$$

Since the input, $u(t)$ is modulated with time periodic signal, here only B matrix is time periodic. We can express B matrix as complex Fourier series in terms of its harmonics as

$$B(t) = \left\{ \ldots, 0, \begin{bmatrix} 0 \\ -\beta \end{bmatrix}, \begin{bmatrix} 0 \\ 1 \end{bmatrix}, \begin{bmatrix} 0 \\ \beta \end{bmatrix}, 0, \ldots \right\} \tag{4.15}$$

If system matrices are examined, only unknown parameter is β. So, for different values of β, harmonic transfer function, $\mathcal{H}(s)$, of the system is computed by using following formula:

$$\mathcal{H}(s) = \mathcal{C}[sI - (\mathcal{A} - \mathcal{N})]^{-1}\mathcal{B} + \mathcal{D}, \tag{4.16}$$

According to the obtained harmonic transfer function, Nyquist diagram is plotted. Here, we show the results of Nyquist stability test for the values of $\beta = [0, 0.5, 0.7]$. Open loop poles of the system are computed as $s_1 = 0$ and $s_2 = -2\zeta$. There is a single right half plane pole at $s = 0$. Therefore, to provide stability of the system, $-k$ point should be encircled in one times in counterclockwise direction. The reason of the encirclement of point $-k$ instead of point $-1/k$, is plotting inverse Nyquist diagram for the sake of clarity. Note that the point k represents the value of a in the lossy Mathieu equation. That is, the obtained range for point

k after applying Nyquist stability test corresponds to the range for the value of a.

Inverse Nyquist diagram of the system for the value of $\beta = 0$ is illustrated in Fig. 4.5 and stability diagram obtained by using Floquet theorem with the line whose slope corresponds to the value of $\beta = 0$ is shown in Fig. 4.6. According to Nyquist stability criterion, to satisfy stability, point $-k$ has to be CCW encircled in one times. If we investigate the Fig. 4.5, in the range of $k > 0$ point $-k$ is encircled in one times. Hence, we can conclude that $k > 0$ provides closed loop stability of the LTP system as $k < 0$ produces unstable configurations. When we compare the results of Nyquist stability test with stability diagram of Floquet theorem illustrated in Fig. 4.6, along the line of $\beta = 0$ on Fig. 4.6 it does not meet with unstable regions which was shown as red region. It shows that the stability results of the Nyquist test is compatible with stability diagram of Floquet theory.

For the value of $\beta = 0.5$, many closed CCW circuit which are symmetrical around the real axis are formed. The points encircled by a CCW circuit generates stable solutions for the Mathieu equation as the points not encircled with a CCW circuit corresponds to the unstable solutions. In Fig. 4.7, the values of feedback gain $k = a$ which provides stable solutions for the lossy Mathieu equation is illustrated with green dot-lines, while the values that results with unstable solutions shown with red dot-lines. The line with slope of $\beta = 0.5$ is plotted on the stability diagram of Floquet theory. If we compare the limit points of the ranges of value of k which provides stable solution obtained by Nyquist diagram illustrated in Fig. 4.7 with the intersect points of the $\beta = 0.5$ line on the stability diagram of Floquet theory shown in Fig. 4.8, we can conclude that stability boundaries are same both on Nyquist stability test and on Floquet theory. Similar results can be concluded from the Fig. 4.9 and Fig. 4.10. The ranges of the red and green dotted lines shown on the Nyquist diagrams consist perfectly with the intersect points boundaries of their corresponding lines on Floquet stability diagram. As a result, we show that the stability boundaries of lossy Mathieu equation can be provided by both of Nyquist diagram and Floquet theory. In Floquet theory, we compute maximum absolute value of eigenvalues of monodromy matrix of LTP system for each point in (q, a) plane. The values which are greater than one are saved as

unstable points while the others registered as stable points. However, in Nyquist stability test, as designing one of the parameter, a, of the system as feedback gain, we find the stability boundaries by looking to the real axis crossings of the closed CCW contours in Nyquist diagram for the line $\beta = q/a$. Stability boundaries obtained by both methods are observed as same. The important point here is that while Floquet theory provides stability analysis for merely single point in the (q, a) plane, Nyquist stability test enables us to analysis stability of LTP system for a line $\beta = q/a$ in the (q, a) plane. In this way, two dimensional stability problem is reduced to the one dimensional stability analysis problem.

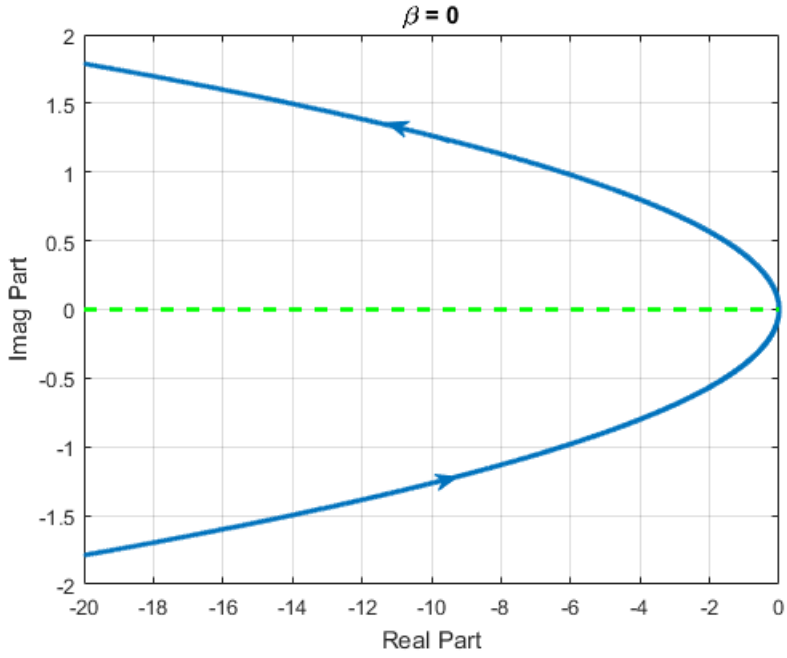

Figure 4.5: Inverse Nyquist diagram of lossy Mathieu equation for $\beta = 0$. Green dot lines shows the stable regions for the value of $k = a$.

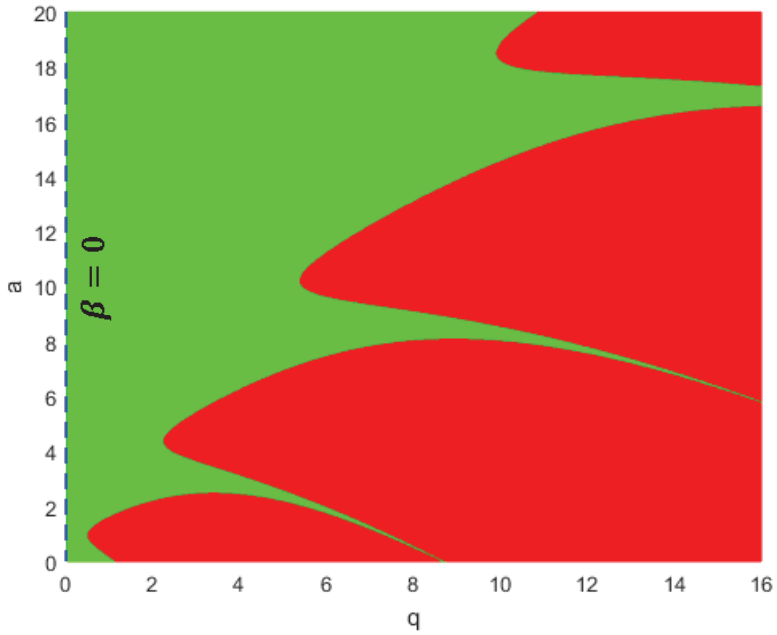

Figure 4.6: Stability diagram obtained by Floquet Theorem of lossy Mathieu equation with the line its slope is $\beta = q/a$.

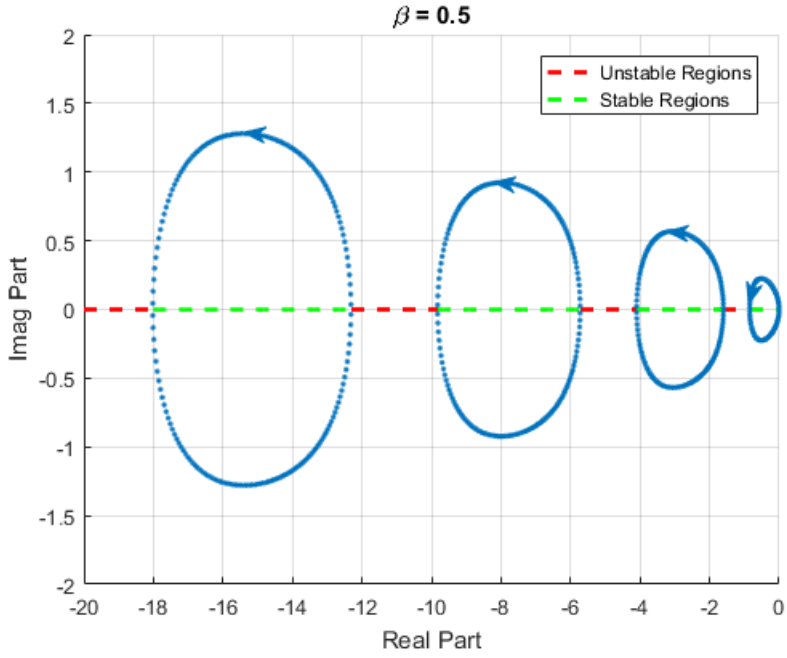

Figure 4.7: Inverse Nyquist diagram for $\beta = 0.5$. Green dot lines shows the stable regions and red lines corresponds to unstable regions for the value of $k = a$.

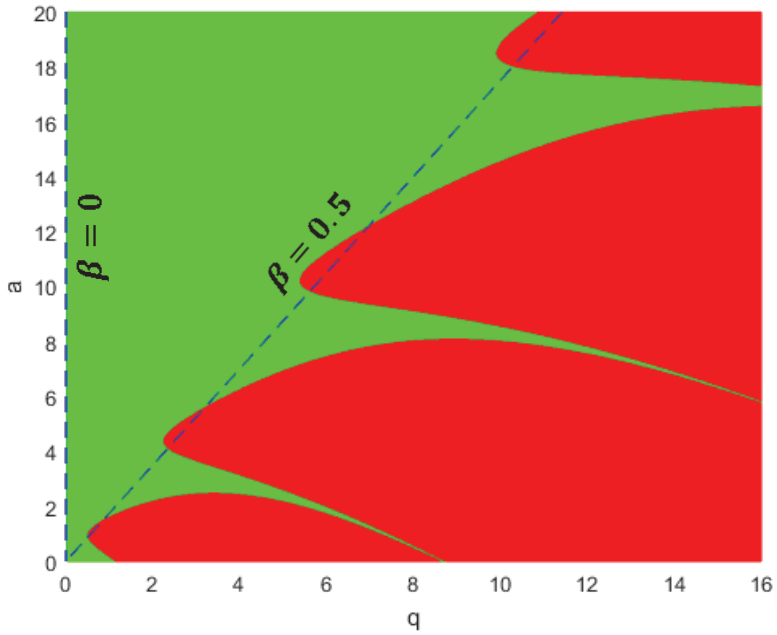

Figure 4.8: Stability diagram obtained by Floquet Theorem of lossy Mathieu equation with the line its slope is $\beta = q/a$.

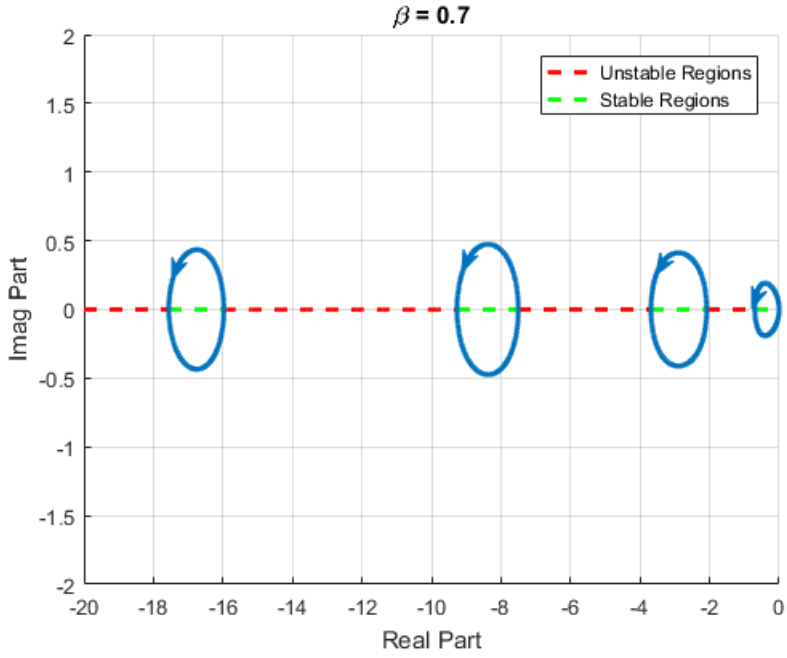

Figure 4.9: Inverse Nyquist diagram for $\beta = 0.7$. Green dot lines shows the stable regions and red lines corresponds to unstable regions for the value of $k = a$.

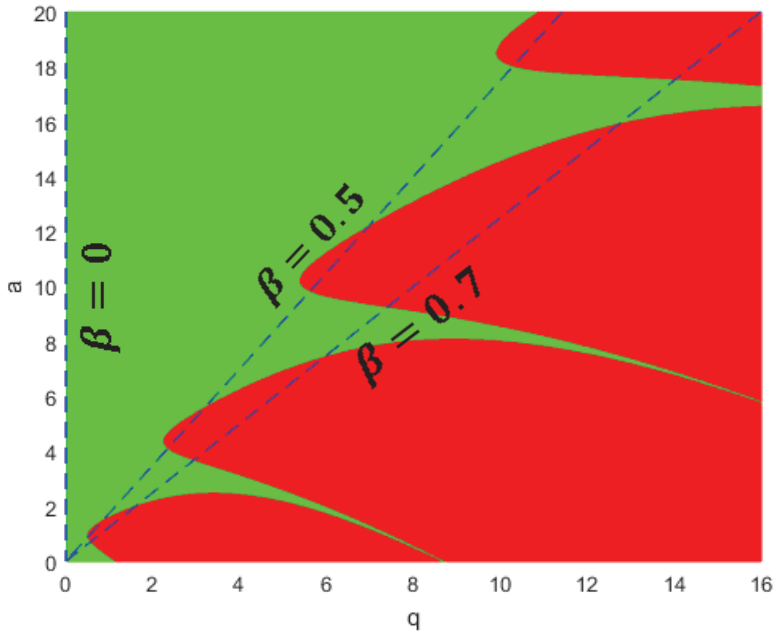

Figure 4.10: Stability diagram obtained by Floquet Theorem of lossy Mathieu equation with the line its slope is $\beta = q/a$.

4.2 Stability Analysis of LTP Systems via Nyquist Criterion with Estimated HTFs with Data-Driven Approach

When we have the state space representation, we can obtain the Nyquist plots, and design controllers accordingly. However, our problem of interest is the unknown LTP systems for which a state space representation may not be available. Therefore, we seek to design a novel methodology, where we can obtain Nyquist plots of unknown LTP systems via input–output data analysis using the concept of harmonic transfer functions. In this section, we show the application of stability analysis with Nyquist criterion by using estimated harmonic transfer functions which is obtained via data-driven system identification method investigated in Section 3.2. In order to obtain Nyquist diagram of LTP systems, we compute the eigenloci of harmonic transfer function by using standard eigenvalue problem on computer. However, there is a difference between the structure of harmonic transfer function which is used in Nyquist diagram and estimated harmonic transfer functions via data-driven system identification approach. Estimated harmonic transfer functions are included in the harmonic transfer function structure which was the source of Nyquist diagram. The relation between estimated HTFs ($\hat{H}_{\pm n}(\omega_f)$) and required HTF structure to obtain Nyquist diagram is shown in Fig. 4.11.

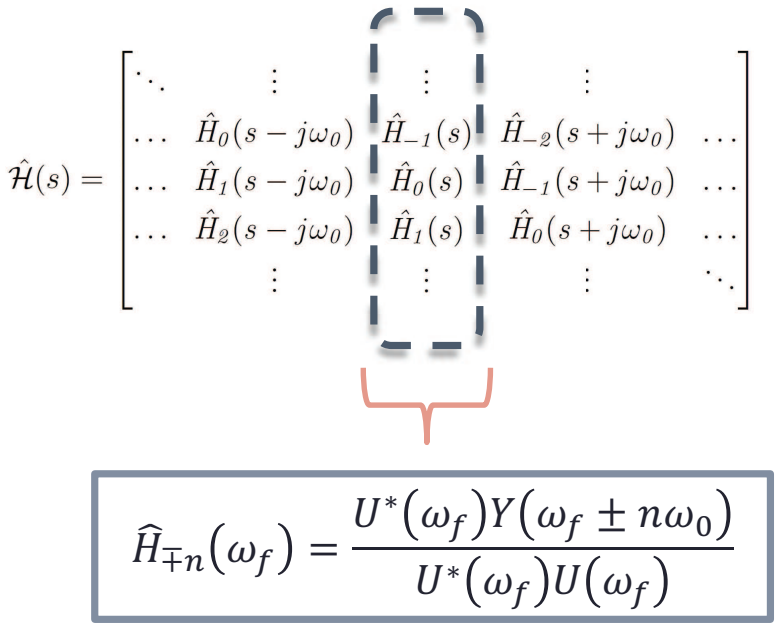

Figure 4.11: The relation between estimated harmonic transfer functions and required harmonic transfer function to plot Nyquist diagram.

Nyquist diagram is plotted based on the eigenloci of the doubly infinite matrix structure illustrated in Fig. 4.11. However, when we apply data-driven system identification methods by using only input-output data in order to obtain estimated harmonic transfer functions of LTP systems, the predicted HTFs, $(\hat{H}_{\pm n}(\omega_f))$, will be as the middle structure taken with a dotted rectangular frame of the doubly infinite HTF matrix as seen in Fig. 4.11. In Nyquist diagram process, the eigenloci of doubly infinite matrix, $\mathcal{H}(s)$, which is truncated to the order of N to be implementable on computer is computed for $s = j\omega$ and ω varying through $-\omega_0/2 < s < \omega_0/2$.

If we look at the structure of HTF matrix shown in Fig. 4.11 which corresponds to the Nyquist diagram, this HTF structure, $\hat{\mathcal{H}}(s)$, includes LTI transfer functions from $\hat{H}_{\pm n}(-\omega_0/2-N\omega_0)$ to the $\hat{H}_{\pm n}(\omega_0/2+N\omega_0)$. However, if we accomplish system identification for $s = j\omega$ and ω varying through $-\omega_0/2 < s < \omega_0/2$, estimated harmonic transfer function consists of LTI transfer functions from $\hat{H}_{\pm n}(-\omega_0/2)$ to the $\hat{H}_{\pm n}(\omega_0/2)$. Therefore, in order to make estimated HTFS suitable for

drawing Nyquist diagram as it will has same structure with $\hat{\mathcal{H}}(s)$, we perform system identification methods for $s = j\omega$ and ω varying through $(\frac{-\omega_0}{2} - N\omega_0)$ to $(\frac{\omega_0}{2} + N\omega_0)$. Then, as placing estimated harmonic transfer functions in this frequency range to their corresponding locations into the HTF structure required in order to obtain Nyquist diagram, we can successfully plot Nyquist diagram with estimated harmonic transfer functions by using input and output data. The main advantage of this procedure is that even if one does not have information about state space model of the LTP systems, one can obtain Nyquist diagram of the system by using estimated harmonic transfer functions via data-driven approach.

4.3 Algorithm for Controller Design Based On HTFs

In this section, our goal is to analyze the stability of LTP systems including controller type of P, PD and PID via Nyquist stability criterion. Here, the main contribution is to design K_p parameter of these controllers as feedback gain and determine range of K_p parameter which stabilizes the system with only one application of Nyquist stability test.

4.3.1 HTF Representation of Controllers

Before we apply Nyquist criterion on the LTP systems including controller, we have to obtain harmonic transfer function of the controller by applying similar approaches to get Toeplitz form of the system matrices of LTP system. However, the controllers designed in this thesis does not have time periodic elements so, they are naturally LTI. For this reason, there is no spectral interactions and harmonic transfer function form of controller can be obtained as [29, 30]:

$$\mathcal{H}_C(s) = \begin{bmatrix} \ddots & \vdots & \vdots & \vdots & \\ \dots & C(s-j\omega_0) & 0 & 0 & \dots \\ \dots & 0 & C(s) & 0 & \dots \\ \dots & 0 & 0 & C(s+j\omega_0) & \dots \\ & \vdots & \vdots & \vdots & \ddots \end{bmatrix} \tag{4.17}$$

where $C(s)$ is transfer function of LTI form controller. In order to apply Nyquist stability analysis which is proposed in Theorem 4.1.1 for LTP systems contained LTI form controller, we have to examine the eigenvalues of multiplication of harmonic transfer function of the plant and HTF of controller which are illustrated in Fig. 4.1. That is, to analyze closed loop stability of the LTP system, eigenvalues of open loop harmonic transfer function of the system including controller, $\mathcal{H}(s) = \mathcal{H}_C(s)\mathcal{H}_P(s)$, are investigated. The closed loop system is stable from input, r, to the output, y if and only if total number of encirclement of point $-1/k$ around counterclockwise (CCW) direction is equal to the number of right half plane poles of open loop system, $\mathcal{H}_C(s)\mathcal{H}_P(s)$.

4.4 Application of Nyquist Criterion with Theoretical HTFs in Controller Design for Unstable Mathieu Example

In this section, our goal is to investigate stability analysis of LTP systems including P, PD and PID controller respectively by using Nyquist stability criterion. According to the results of stability analysis of LTP systems with controller, we will acquire gain margin (GM) and phase margin (PM) of the system with respect to parameters of controllers. As a results of these measurements, we determine some controllers which enhance the performance of the system and we make simulation with chosen controllers in order to show the performance of the controllers in time domain.

In order to implement these procedures, we use the lossy Mathieu example

whose system matrices are given in the sequel.

$$A(t) = \begin{bmatrix} 0 & 1 \\ -(5 - 8cos\omega_0 t) & -2\zeta \end{bmatrix},$$

$$B = \begin{bmatrix} 0 \\ 1 \end{bmatrix}, \quad C = \begin{bmatrix} 1 & 0 \end{bmatrix}. \tag{4.18}$$

The parameters of this system are chosen as $\omega_0 = 2$ and $\zeta = 0.2$. The poles of open loop system in s plane are obtained as $s_1 = 0.3931$ and $s_2 = -0.7931$ by computing eigenvalues of $\mathcal{A} - \mathcal{N}$ in fundamental strip. This system has one pole at right half plane.

4.4.1 P type Controller

The lossy Mathieu equation in (4.18) is unstable with the parameters given above since it includes one pole at right half plane. In order to make system stable, P type controller can be designed by using Nyquist criterion. According to Theorem 4.1.1, since the system has one pole at right half plane, the closed loop system is stable if and only if $-1/k$ point is encircled in one times around CCW direction. In order to calculate K_p values of P controller which stabilizes the system, harmonic transfer function of the LTP system, $\mathcal{H}_p$ is computed as in equation (2.33) and Nyquist diagram of $\mathcal{H}_p$ is obtained as in the Fig. 4.12.

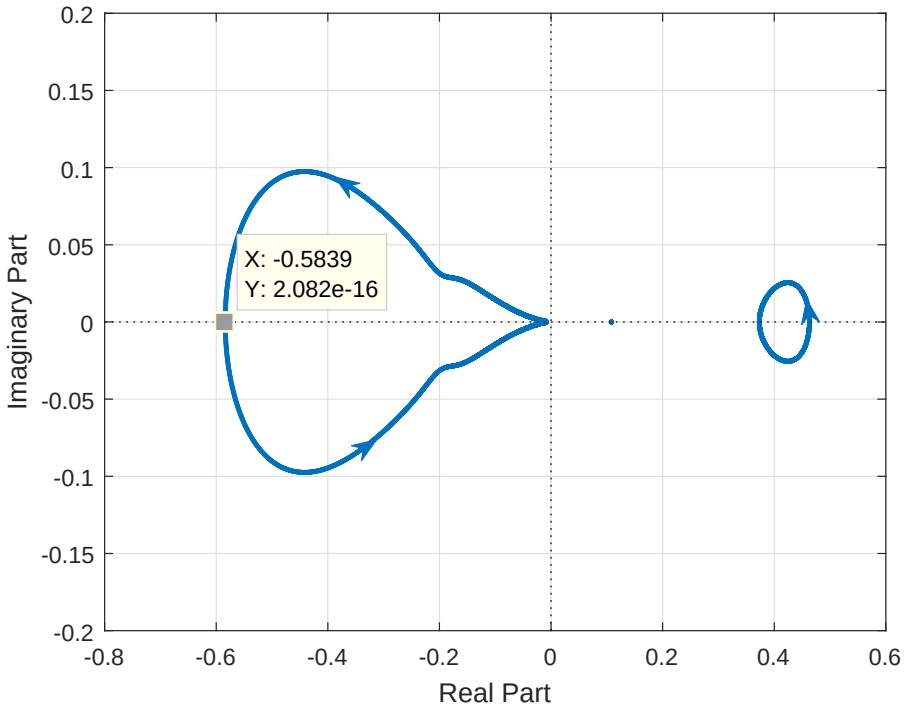

Figure 4.12: Nyquist diagram of open loop harmonic transfer function, $\mathcal{H}_p$.

In the nyquist diagram of lossy Mathieu equation shown in Fig. 4.12, negative real axis is encircled counterclockwise one times for the values of $-1/k \in [-0.58, 0]$. Hence, the range of K_p values which stabilize the closed loop system is computed as $[1.71, \infty)$.

According to the values of K_p that stabilizes the system, gain and phase margin graphics of the closed loop system is given in Fig. 4.13 with **A** and **B** respectively. Gain margin for the closed loop system can be defined by how much gain can be applied without destabilizing the closed loop system. In order to calculate phase margin of the system with respect to K_p value, we first draw a circle centered at origin with $-1/K_p$ radius. Then, we found the point, p_0, which intersects the Nyquist plot with the circle. The angle from the negative real axis to the intersect point, p_0, gives us the phase margin. If we investigate gain and phase margins of the closed loop system with respect to K_p, as gain margin changes between $(0.01, 1]$, phase margin varies between $(2^\circ, 13^\circ]$. However, the phase margin of

the closed loop system does not vary much and as it can be seen from Fig. 4.13-B the phase margin is not sufficiently high. Therefore, in order to both enhance the performance and stabilize the system, alternative controllers can be designed and the performances of these controllers on the system can be investigated.

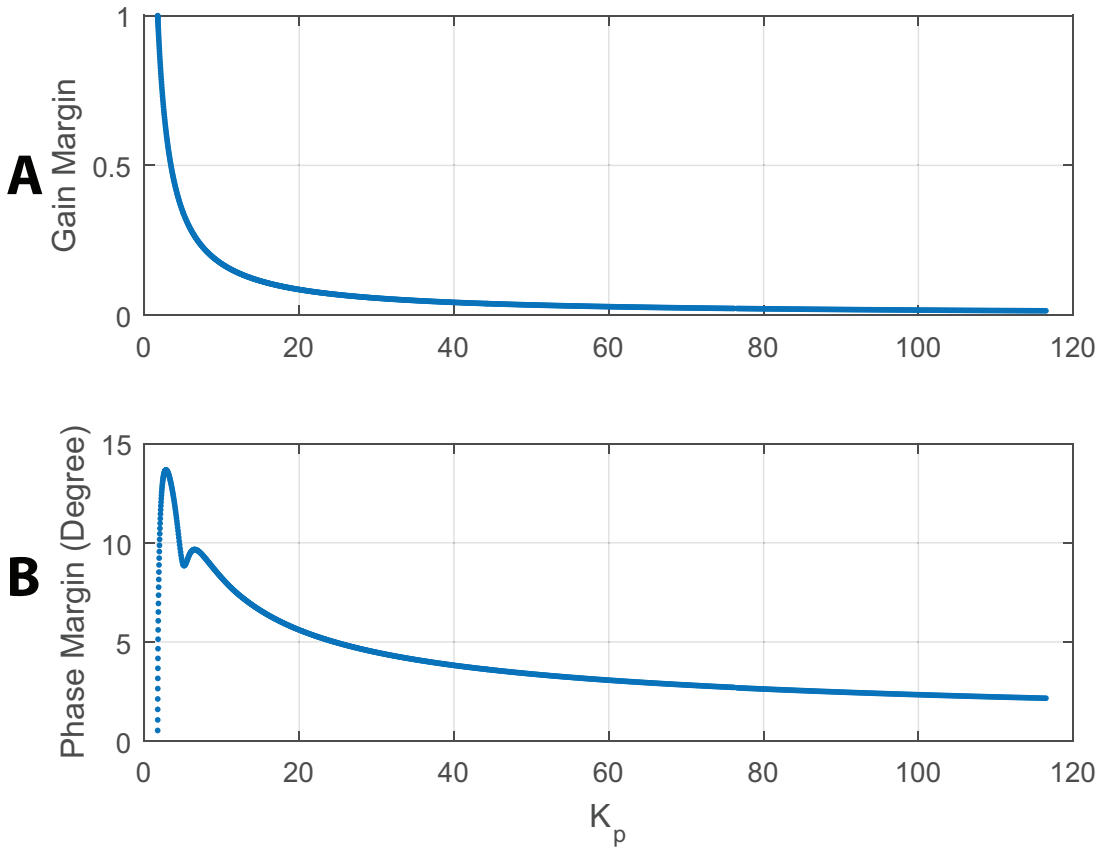

Figure 4.13: Gain (A) and Phase (B) margin graphs with respect to the K_p values which stabilize the system.

4.4.2 PD type Controller

The main objective of this section is to design a PD controller which stabilize the unstable LTP system and enhance the performance of the system in terms of phase and gain margins. Primarily, we illustrate how to adapt structure of PD controller into the closed loop feedback system which is shown in Fig. 4.1.

PD controller structure is given as:

$$\begin{aligned} C_{pd}(s) &= K_p + K_d s \\ &= K_p \underbrace{(1 + \alpha s)}_{C(s)} \end{aligned} \tag{4.19}$$

where $\alpha = K_d/K_p$. By using LTI $C(s)$, HTF form of the controller is obtained as illustrated in (4.17). Here, the reason behind extracting K_p parameter from the HTF form of controller is to design K_p parameter as feedback gain as it is shown in Fig. 4.1 and thus, for different values of α, by applying Nyquist stability test to compute the range of K_p which stabilizes the closed loop system. The important point is as designing K_p parameter of PD controller as feedback gain and applying Nyquist stability test provides stability analysis along the line $\alpha = K_d/K_p$ with one test instead of making stability analysis for the single point in (K_p, K_d) plane. Hence, two dimensional stability problem which depends on the points in (K_p, K_d) plane can be reduced successfully to the one dimensional stability analysis problem as investigating stability along the line of $\alpha = K_d/K_p$.

4.4.2.1 Stability Analysis and Performance of the System with respect to K_p and K_d Parameters

In this section, we first analyze the stability of LTP unstable Mathieu example given in Section 4.4 with respect to (K_p, K_d) controller parameters via Nyquist stability criterion. We then obtain gain and phase margin graphs of closed loop system according to the (K_p, K_d) parameters which stabilize the unstable system. For the different values of $\alpha = K_d/K_p$ between $[0.01, 100]$ changing with 0.01 steps, we apply Nyquist stability test and the value range of K_p that stabilize the closed loop system. By using $K_d = \alpha K_p$ equity, we also calculate the value range of K_d. According to this, we obtain the Fig. 4.14 which includes stable and unstable regions with respect to (K_p, K_d) via Nyquist stability criterion.

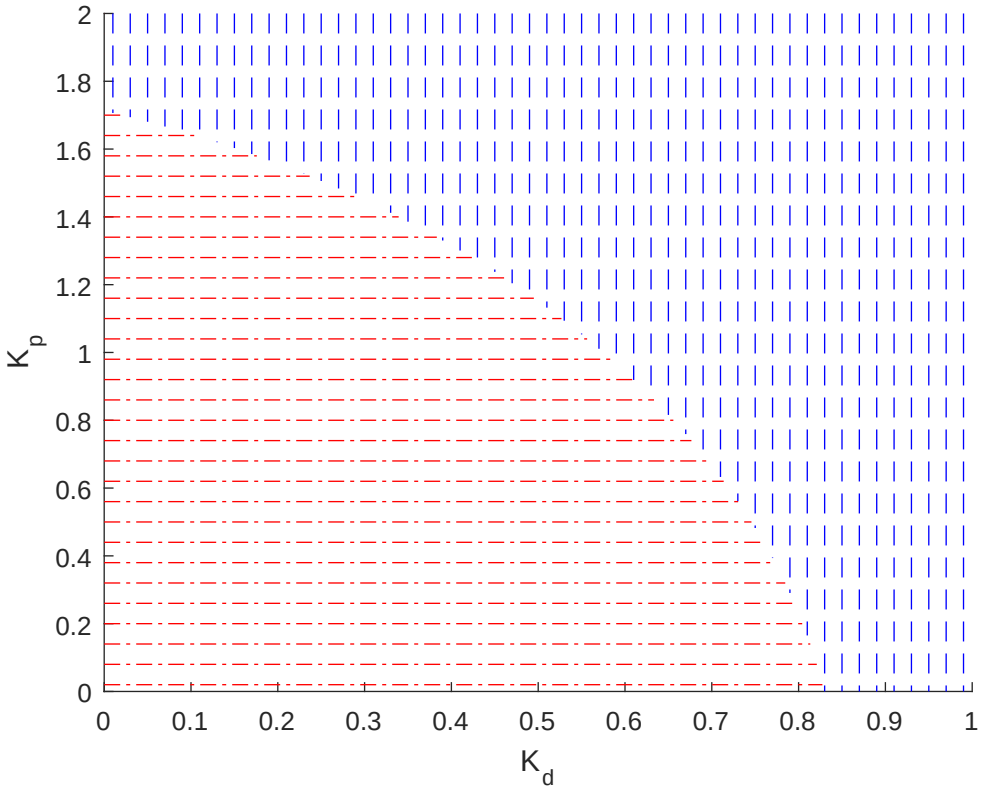

Figure 4.14: Stable and unstable regions of closed loop system with respect to the value of K_p and K_d. Red (horizontally dashed) lines illustrate unstable regions and blue (vertically dashed) lines include stable regions of closed loop system.

In Fig. 4.14, blue (vertically dashed) lines illustrate the region where closed loop system is stable for corresponding (K_p, K_d) and red (horizontally dashed) lines includes the controller parameters which leave the system as unstable. An significant point is that closed loop stability analysis of LTP system with controller is achieved along the line $\alpha = K_d/K_p$ changing α between $[0.01, 100]$ by designing K_p parameter as feedback gain instead of a single point in (K_p, K_d) plane. After determining (K_p, K_d) values which make the closed loop system stable, for the purpose of investigating the performance of the system, we compute the gain and phase margins of the system with controller by using Nyquist diagrams. Thus, we aim to test a PD controller having (K_p, K_d) parameters which may provide a possible performance improvement for the system given by damped

Mathieu equation. In this respect, the three dimensional (3D) graphs of gain and phase margins of the closed loop system with respect to the value of (K_p, K_d) parameters that stabilize the system are given in Fig. 4.15 and Fig. 4.16 accordingly. In these figures, while x axis corresponds to K_p values, y axes belongs to K_d values of PD controller. The gain and phase margin values are shown via color map. The red regions illustrated in Fig. 4.15 and Fig. 4.16 belongs to the unstable regions which are shown in Fig. 4.14.

If we examine the Fig. 4.15, the gain margin has high values in the locations where K_p and K_d close to the origin. However, phase margin increases in the regions where K_d also increases. According to this, it can be concluded that there is a trade-off between gain and phase margin.

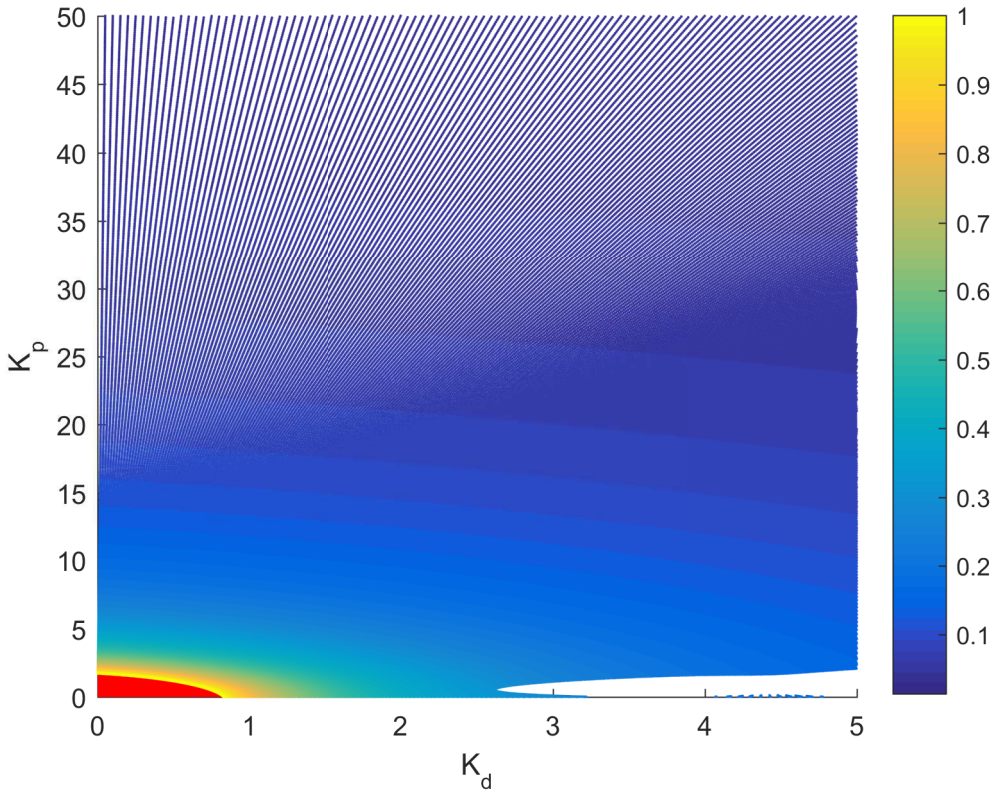

Figure 4.15: Gain margin of closed loop system with respect to K_p and K_d values. Red region illustrates the unstable regions.

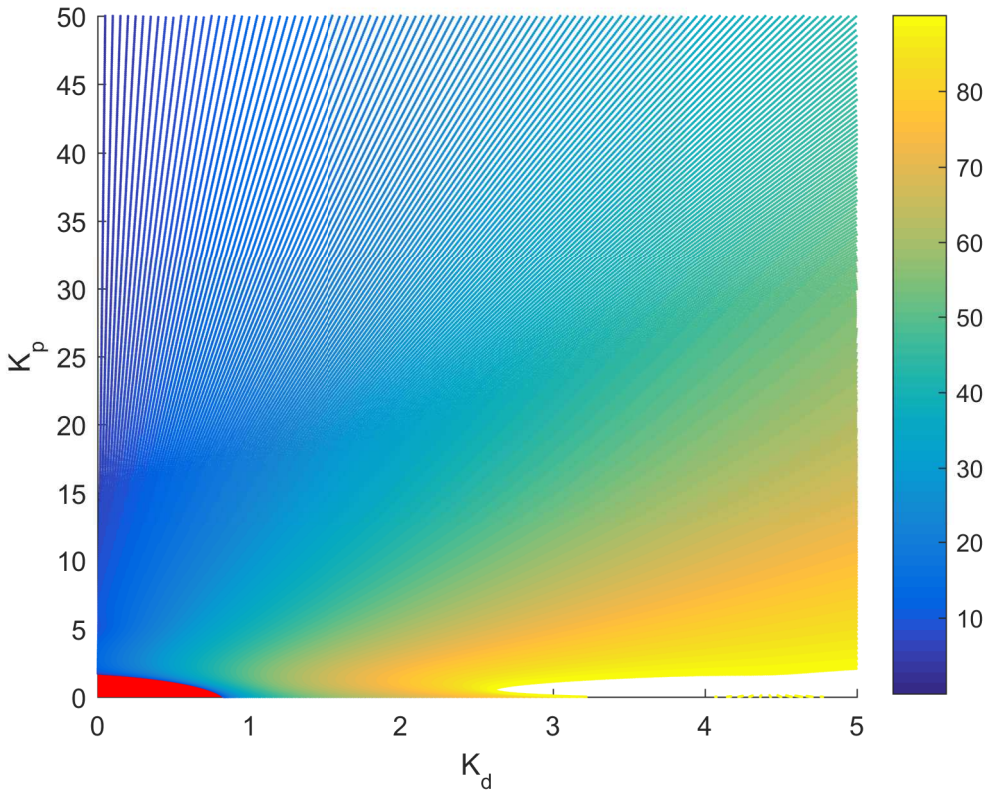

Figure 4.16: Phase margin of closed loop system with respect to K_p and K_d values. Red region illustrates the unstable regions.

When gain and phase margins are taken into consideration, as gain margin and phase margin will be between $[0.25, 0.6]$ and $[40°, 90°]$ respectively, we design two different PD controllers which yield phase and gain margins close to the boundaries of these ranges.

The first controller is given as:

$$C_{PD_1}(s) = 2.3 + 0.75s \tag{4.20}$$

where resulting gain and phase margin are obtained as:

Gain Margin:(GM) 0.55 **Phase Margin:**(PM) 43°

The second controller is given as:

$$C_{PD_2}(s) = 1.6 + 3s \tag{4.21}$$

where resulting gain and phase margin are obtained as:

Gain Margin:(GM) 0.27 **Phase Margin:**(PM) 87°

4.4.2.2 Time Domain Simulations with C_{PD_1} and C_{PD_2}

In this section, we evaluate the performance of PD controllers which are designed in (4.20) and (4.21) in terms of percentage overshoot (PO), rising time (T_r) and settling time (T_s) criterion. In these simulations, the input is equal to the zero and corresponding output is x. Time domain simulation results of C_{PD_1} and C_{PD_2} which are designed regarding gain and phase margin graphs are illustrated in Fig. 4.17 and Fig. 4.18 accordingly.

Controller (PD)	GM	$PM(^\circ)$	$PO(\%)$	$T_r(sn)$	$T_s(sn)$
$2.3 + 0.75s$	0.55	43	29	1.5	9.33
$1.6 + 3s$	0.25	87	2	1.7	2.3

Table 4.1: The performance of C_{PD_1} and C_{PD_2} in time domain simulations

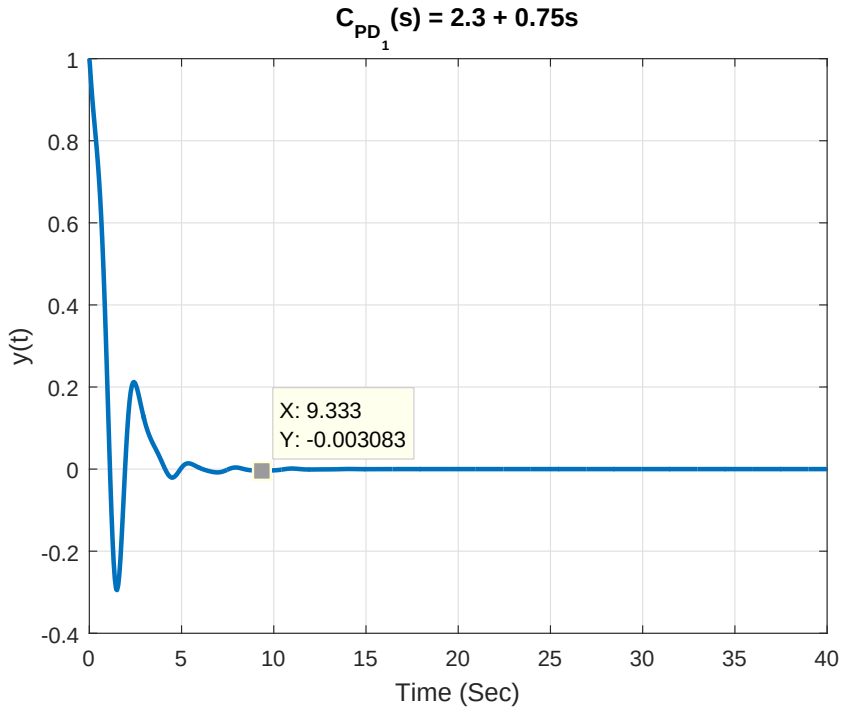

Figure 4.17: Output response of closed loop unstable system including $C_{PD_1} = 2.3 + 0.75s$ controller in time domain.

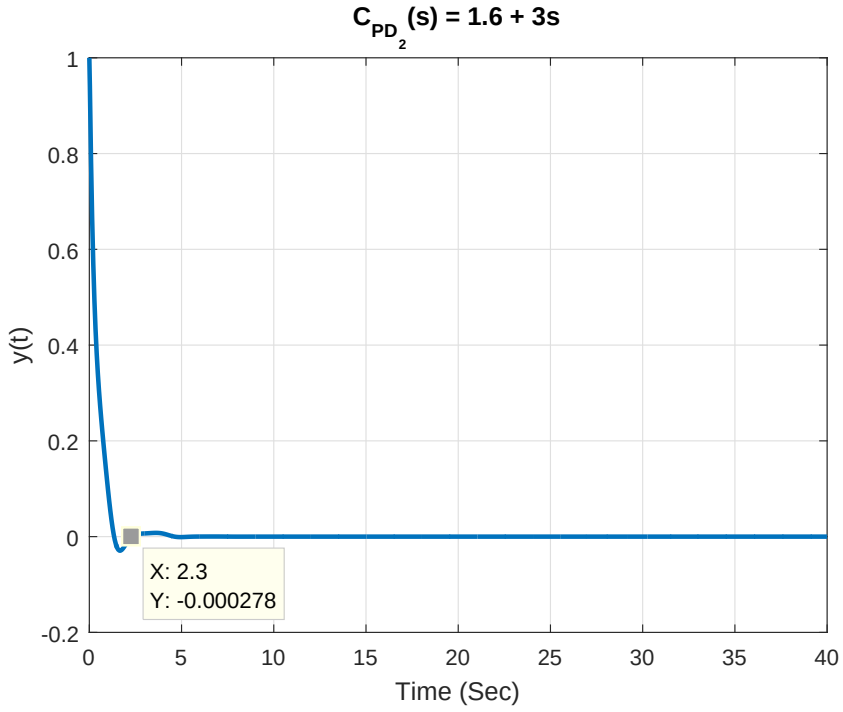

Figure 4.18: Output response of closed loop unstable system including $C_{PD_2} = 1.6 + 3s$ controller in time domain.

We observe that when the K_d increases, the phase margin increases and the time domain simulations show that the percentage overshoot and settling time also decreases. However, as a trade off, the gain margin decreases. We design two different PD controllers which successfully stabilize and enhance the performance of LTP systems. However, if there is a external disturbance in the LTP system, PD controller cannot be sufficient in order to reject the disturbance and provide zero tracking error. In order to test the behavior of the system with PD controller in the existence of disturbance, we insert external step input disturbance at 20^{th} seconds. The output of the LTP system with C_{PD_2} is illustrated in Fig. 4.19. As it is seen in Fig. 4.19, PD controller cannot be sufficient in order to reject

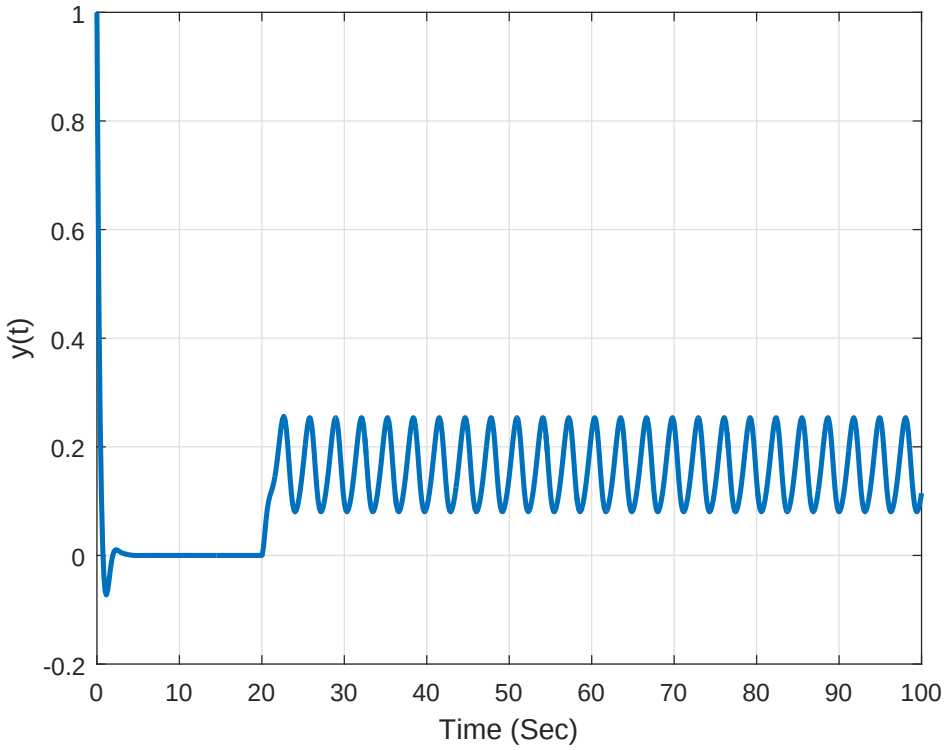

Figure 4.19: Output response of LTP System with C_{PD_2} in the existence of step input disturbance which is applied at 20^{th} seconds.

step input disturbance and make tracking as zero. After we apply step input disturbance, output response of the system behaves as periodic signal.

4.4.3 PID type Controller

In this section, we aim to design PID controller in order to stabilize and enhance the performance of LTP systems. Besides, by adding integrator to a controller we can achieve both zero tracking error and constant disturbance rejection [59, 60]. Hence, using PID controller to stabilize the LTP system provides constant disturbance rejection in the existence of any external disturbance. The structure of the PID controller is as given below:

$$\begin{aligned} C_{pid}(s) &= K_p + \frac{K_i}{s} + K_d s \\ &= K_p \underbrace{(1 + \frac{\alpha_1}{s} + \alpha_2 s)}_{C(s)} \end{aligned} \tag{4.22}$$

where $\alpha_1 = K_i/K_p$ and $\alpha_2 = K_d/K_p$.

To investigate stability of the LTP system with PID controller, we can apply similar procedure with PD controller. Here by designing K_p parameter as feedback gain, for different values of (α_1, α_2), we can apply Nyquist stability test and find the range for K_p, K_i and K_d parameters which stabilize the system. We illustrate the time domain simulation results of sample PID controller on the lossy Mathieu example given in equation (4.18) with and without step input disturbance. A sample PID controller is given below:

$$C_{pid}(s) = 5(1 + \frac{1}{s} + 1.8s). \tag{4.23}$$

We note that with this controller, the closed-loop system is stable. The response of the system with this controller without disturbance is shown in Fig. 4.20. As percentage overshoot, PO, of the closed loop system is equal to 9%, settling time, T_r is observed as 4.5 *sec*.

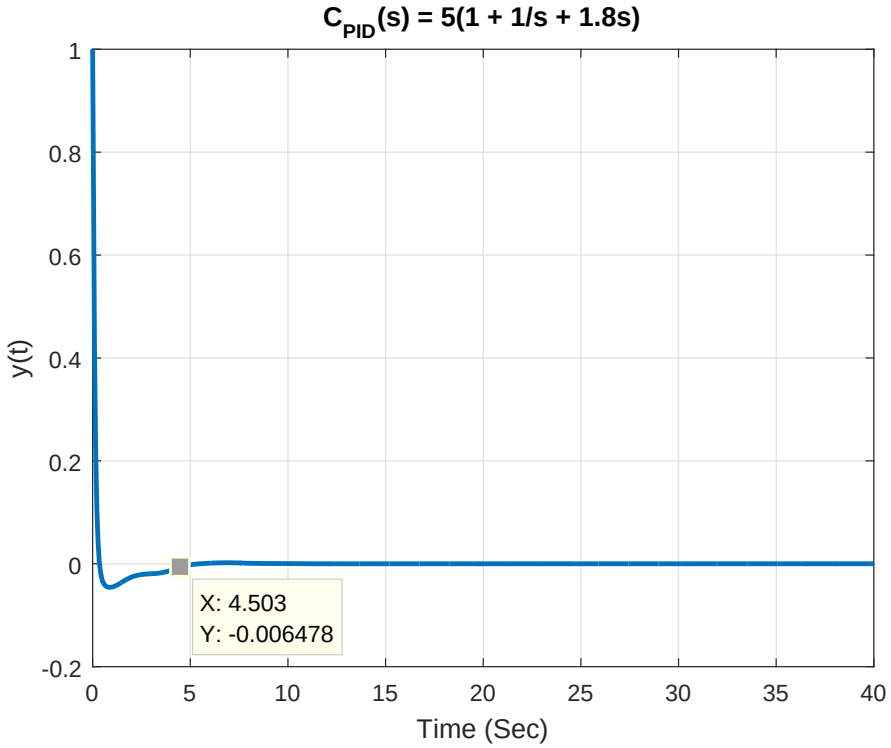

Figure 4.20: Output response of LTP System with $C_{PID} = 5(1 + \frac{1}{s} + 1.8s)$.

Time domain simulation of PID and PD controller provide similar results in terms of percentage overshoot, PO, and settling time, T_r. In order to demonstrate the advantage of PID controller, we repeat the time domain simulation of the system in the existence of step input disturbance. The Fig. 4.21 shows the output response of the system with PID controller under the presence of step input disturbance. As expected, PID controller can successfully reject the step input disturbance and yield steady state error zero.

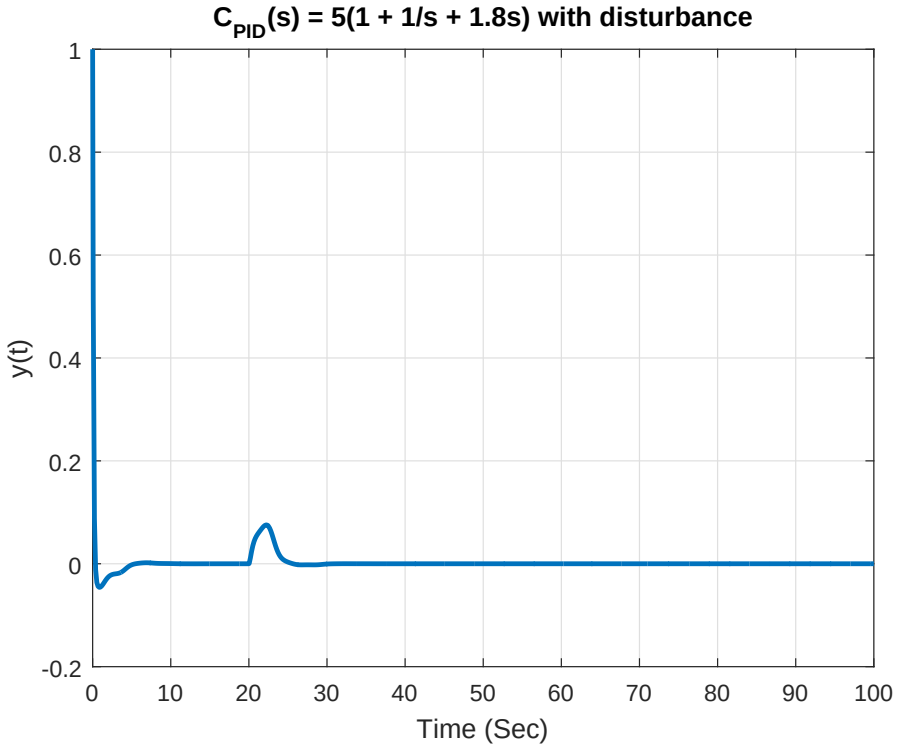

Figure 4.21: Output response of LTP System with $C_{PID} = 5(1 + \frac{1}{s} + 1.8s)$ in the existence of step input disturbance which is applied at 20^{th} seconds.

4.5 Application of Nyquist Criterion with Estimated HTFs in Controller Design for Stable Mathieu Example

In this section, we illustrate the design of controller in order to enhance the performance of stable Mathieu example by using the Nyquist diagram of estimated harmonic transfer functions which is obtained with sum of cosine input signal and its corresponding data. The system matrices of stable lossy Mathieu equation is given in the sequel:

$$A(t) = \begin{bmatrix} 0 & 1 \\ -(5 - 4cos\omega_0 t) & -2\zeta \end{bmatrix},$$

$$B = \begin{bmatrix} 0 \\ 1 \end{bmatrix} \quad C = \begin{bmatrix} 1 & 0 \end{bmatrix}, \tag{4.24}$$

The parameters of this system are chosen as $\omega_0 = 2\pi$ and $\zeta = 0.2$. The poles of open loop system in s plane are obtained as $s_1 = -0.2 - 2.2271i$ and $s_2 = -0.2 + 2.2271i$ by computing eigenvalues of $\mathcal{A} - \mathcal{N}$ in fundamental strip. Note that this system is stable since it has no pole at right half plane.

Since this system is stable, we can estimate the harmonic transfer function by using data-driven system identification methods. For this example, we first estimate the HTFs of the system, then we modify it in order to obtain HTF structure illustrated in Fig. 4.11 which is required to obtain Nyquist diagram. The important point here is that we do not have any information about the state space model of the example, we only have the exciting input signal and their corresponding outputs. Here, the Nyquist diagram of stable Mathieu example which is obtained from eigenloci of estimated harmonic transfer functions by using input output data is shown in Fig. 4.22.

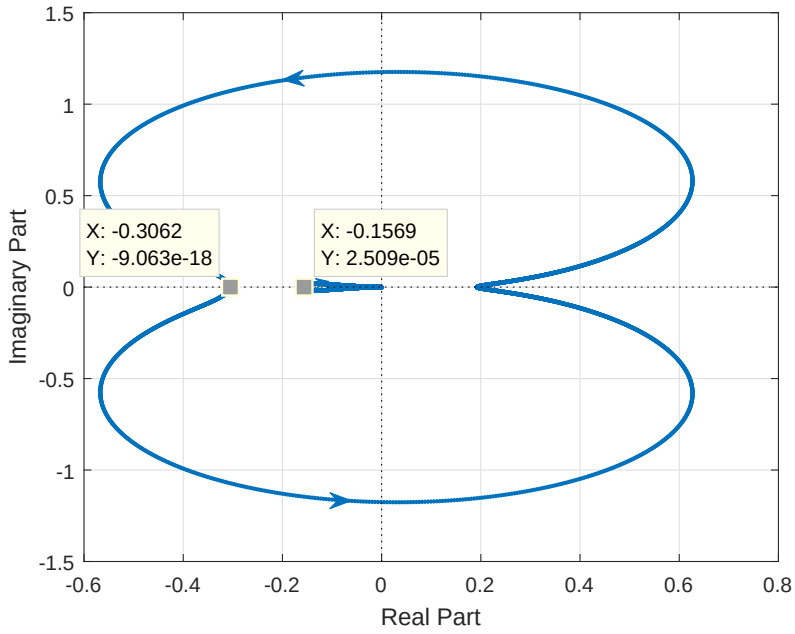

Figure 4.22: Nyquist diagram of stable Mathieu equation which is obtained from eigenloci of estimated harmonic transfer function.

When we investigate the Nyquist diagram of stable Mathieu example, there are two points cross the real axis at left half plane where -0.3062 and -0.1569. According to Theorem 4.1.1, in order to satisfy stability, $-1/k$ point should not be encircled in CCW since it has no pole at right half plane. Regarding this, stabilizing feedback gain values are obtained as below:

$$0 < k < 3.33 \quad \text{and} \quad 6.37 < k < \infty \tag{4.25}$$

The open loop output response of stable Mathieu equation is illustrated in Fig. 4.23.

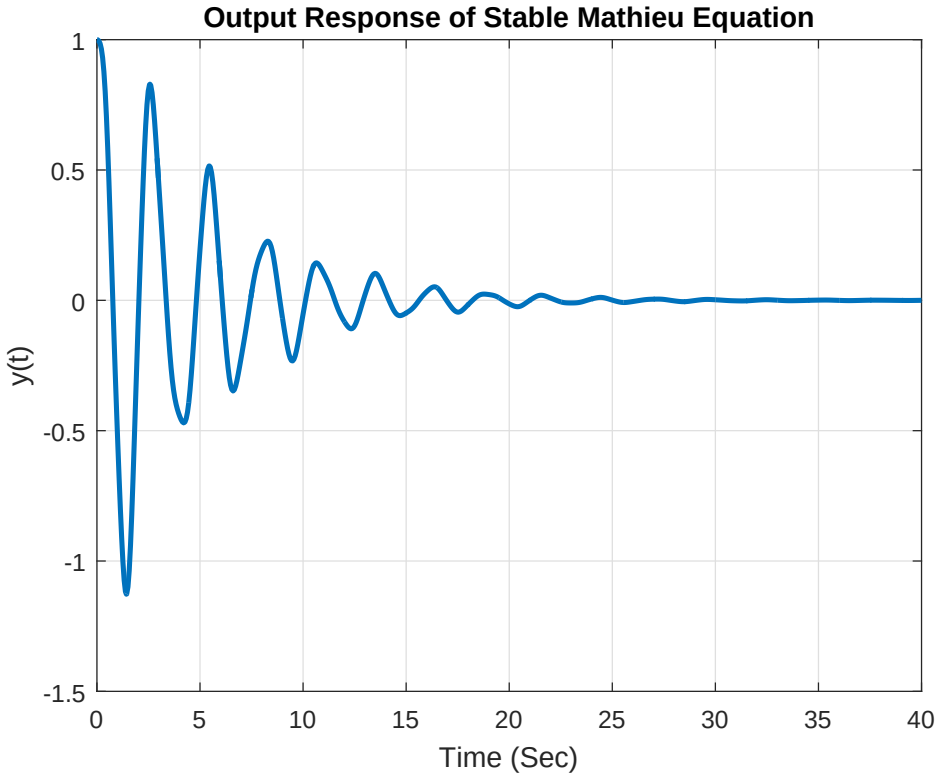

Figure 4.23: Output response of open loop stable Mathieu equation in time domain with input zero.

If we investigate the time domain performance of open loop stable Mathieu equation, as percentage overshoot is obtained as $PO = 108\%$, settling time is acquired as $T_s = 24\,sec.$. In order to enhance the performance of this system, we also design PD controllers by using the procedure explained in (4.19) by using

corresponding Nyquist diagram. To investigate the robustness and performance of the system, we obtain the gain and phase margins of the system via Nyquist diagram which is plotted according to estimated harmonic transfer function with respect to parameters of PD controller. The three dimensional (3D) graphs of gain and phase margins of the closed loop system with respect to the value of (K_p, K_d) parameters is illustrated in Fig. 4.24 and Fig. 4.25 respectively.

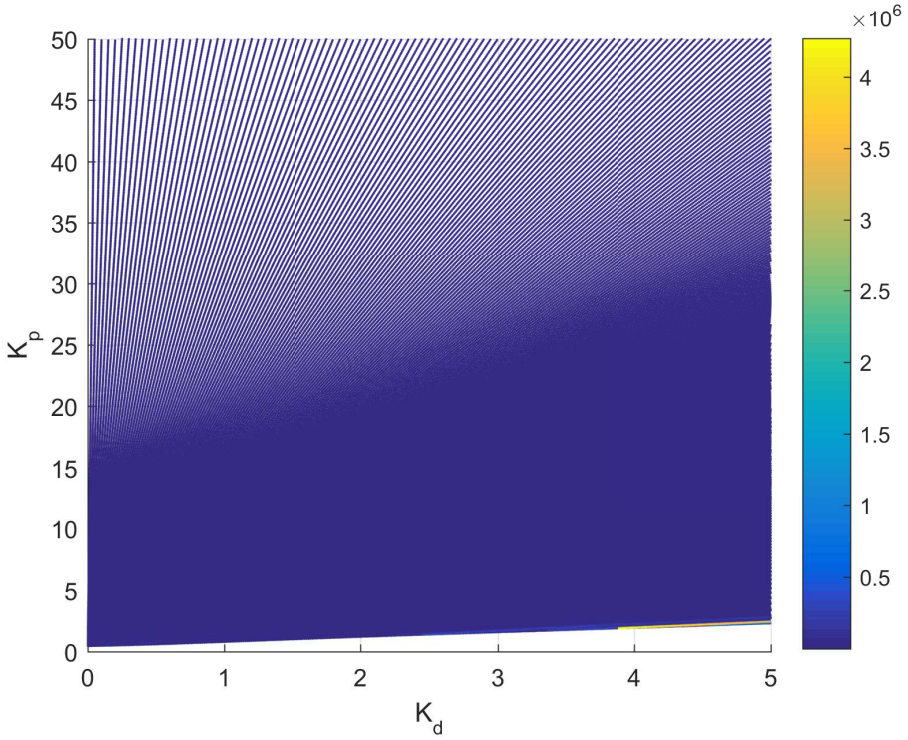

Figure 4.24: Gain margin of closed loop stable Mathieu system with respect to K_p and K_d values.

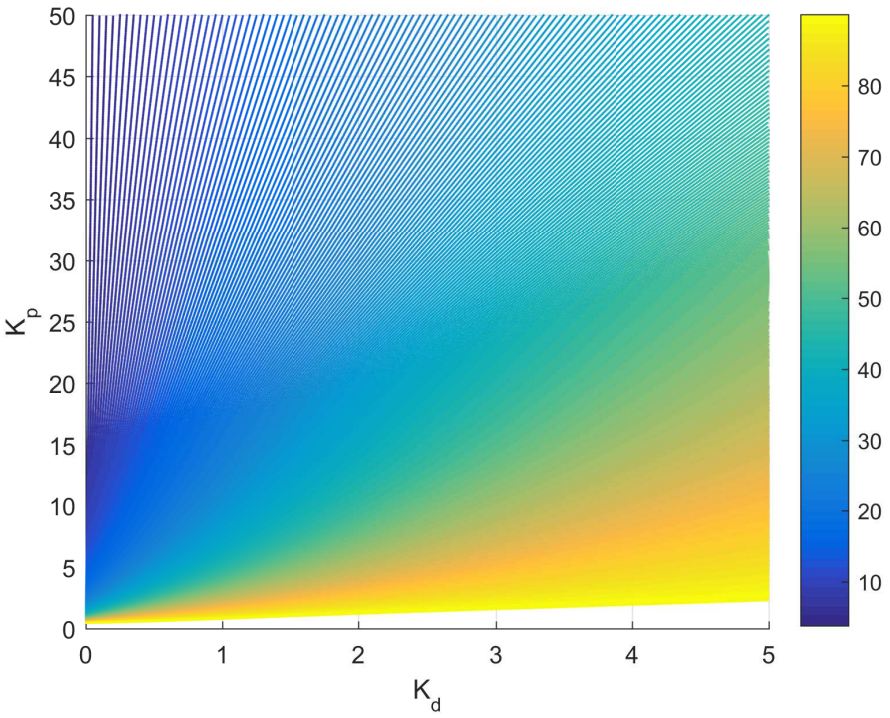

Figure 4.25: Phase margin of closed loop stable Mathieu system with respect to K_p and K_d values.

According to the obtained gain and phase margin graphs, gain margin and phase margin will be between $[0.6, \gg 1]$ and $[40°, 90°]$ respectively. Then, we design two different PD controllers which yield phase and gain margins close to the boundaries of these ranges. The first controller is chosen as:

$$C_{PD_1}(s) = 5 + 3s \tag{4.26}$$

where resulting gain and phase margin are obtained as:

Gain Margin:(GM) 80 **Phase Margin:**(PM) 75°

The second controller is chosen as:

$$C_{PD_2}(s) = 2.4 + 5s \tag{4.27}$$

where resulting gain and phase margin are obtained as:

Gain Margin:$(GM) > 10^6$ **Phase Margin:**(PM) 89°

Here, we evaluate the performance of PD controllers which are designed in (4.26) and (4.27) in terms of percentage overshoot (PO), rising time (T_r) and settling time (T_s) criterion. Time domain simulation results of C_{PD_1} and C_{PD_2} which are designed regarding gain and phase margin graphs are illustrated in Fig. 4.26-A and Fig. 4.26-B respectively.

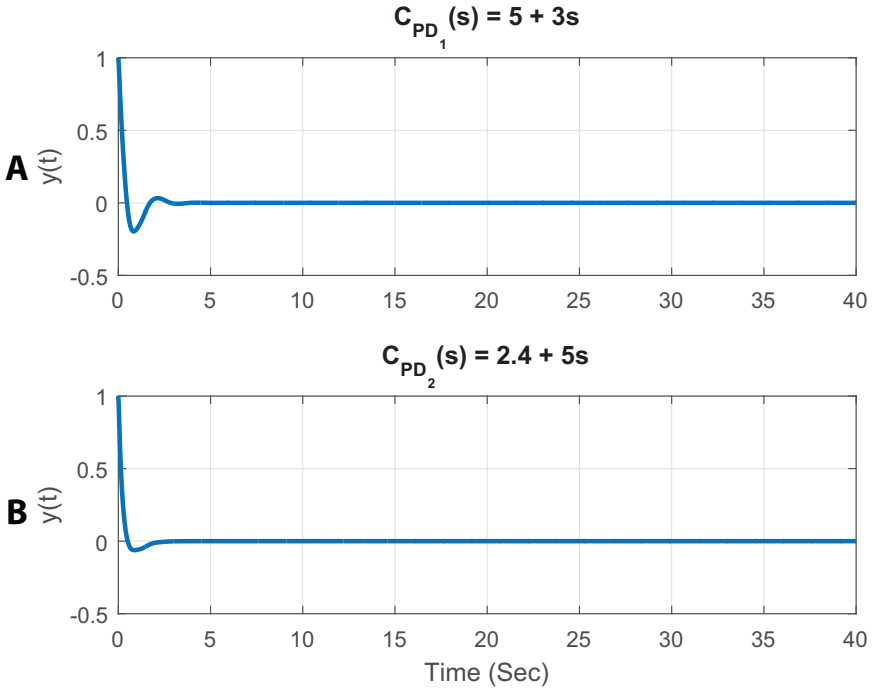

Figure 4.26: Output response of C_{PD_1} and C_{PD_2} in time domain simulations.

Controller (PD)	GM	$PM(^\circ)$	$PO(\%)$	$T_r(sn)$	$T_s(sn)$
$5+3s$	$\gg 1$	75	19	0.8	3.5
$2.4+5s$	$\ggg 1$	89	5	0.9	1.9

Table 4.2: The performance of C_{PD_1} and C_{PD_2} in time domain simulations.

If we compare the closed loop time domain simulation results of stable Mathieu example including PD controller with time domain simulation of open loop stable

Mathieu example, we can conclude that thanks to controllers stability robustness and performance of the system is enhanced regarding percentage overshoot and settling time criterion. As a result, by using only input and output data of stable Mathieu example, we obtain the harmonic transfer function. Then, by applying Nyquist test via estimated harmonic transfer function, we design two different PD controllers which can achieve successful results about increasing the robustness and enhancing the performance of stable system.

Chapter 5

Conclusion

Many important systems encountered in nature such as wind turbines, helicopter rotors, power networks or nonlinear systems which are linearized around their periodic orbits can be modeled as linear time periodic (LTP) systems. Such systems have been intensively analyzed and discussed in the literature with an analytical point of view. However, there are only a few methods in the literature to identify LTP systems using input/output measurements. In particular, due to acquiring analytical solutions for LTP systems are considerably challenging the utilization of experimental data may be preferable regarding identification, analysis and stabilization of such systems . In order to achieve this goal, the use of harmonic transfer functions (HTFs) may be quite helpful.

In this respect, in the first part of this thesis, we aim to obtain harmonic transfer functions of LTP systems via data-driven approach by using only input and output data. In order to achieve that we first explain the frequency domain identification method of [6] which used chirp signal as an input data and estimate the harmonic transfer function via power and cross spectral density functions. Because of the fact that this methodology provides incorrect results in some frequency regions illustrated in [41], we secondly show the identification procedure of HTFs by using single cosine input signal with a specific frequency. However, it

requires multiple experiments in order to cover desired frequency range. Therefore, we lastly propose a formula for the sum of cosine input signal including different frequencies which their output components do not coincide. Finally, we compare the prediction performance of these three identification procedure with the theoretical HTFs for a simple legged model. We showed that prediction performance of single cosine and sum of cosine input signals are similar to the theoretical HTFs even in the frequency ranges where the chirp input signal gives incorrect results.

In the second part of this thesis, we considered the stability analysis and control of LTP systems via harmonic transfer functions. In this regard, we initially, investigate the Nyquist stability criterion of LTP systems which is obtained from eigenloci of HTFs. By using this criterion, we implement the lossy Mathieu equation example given in [20] and analyze the stability of this example with respect to system parameters. Thanks to this criterion, by designing one of the parameters of the system as a feedback gain, we can analyze the stability for a family of gain parameters instead of a single value of gain parameter. From this point of view, we design P, PD and PID controllers which stabilize and enhance the performance of the unstable LTP system by using Nyquist diagram of HTFs. Finally, for the stable LTP system, we estimate the harmonic transfer function by using only input and output data and design PD controllers in order to enhance the performance and increase the robustness. We illustrate the performance results of these controllers in time domain simulations.

As a future work, data driven system identification techniques presented in the thesis can be applied for the analysis and control of various physical systems such as legged robots to improve various performance measures. We believe that the techniques proposed in this thesis will pave the way towards identification of different kind of LTP systems including some physical systems such as legged robots as well as biological rhythmic locomotor systems. Especially, our methodology for designing controllers based on data-driven Nyquist plots allow controller design for performance enhancement in unknown stable LTP systems. One close future application would be identification of harmonic transfer functions for a legged robotic systems such as the one in [38] and ensure optimal convergence to

limit cycle by optimizing performance metrics via data-driven Nyquist plots even if we have do not know its state space structure.

Bibliography

[1] G. S. Bir and K. Stol, "Operating modes of a teeter-rotor wind turbine," tech. rep., National Renewable Energy Lab., Golden, CO (US), 1999.

[2] K. Stol, M. Balas, G. Bir, *et al.*, "Floquet modal analysis of a teetered-rotor wind turbine," *Transactions-American Society Of Mechanical Engineers Journal Of Solar Energy Engineering*, vol. 124, no. 4, pp. 364–371, 2002.

[3] M. S. Allen, M. W. Sracic, S. Chauhan, and M. H. Hansen, "Output-only modal analysis of linear time-periodic systems with application to wind turbine simulation data," *Mechanical Systems and Signal Processing*, vol. 25, no. 4, pp. 1174–1191, 2011.

[4] J. Dugundji and J. H. Wendell, "Some analysis methods for rotating systems with periodic coefficients," *AIAA journal*, vol. 21, no. 6, pp. 890–897, 1983.

[5] S. Hwang, *Frequency Domain System Identification of Helicopter Rotor Dynamics Incorporating Models With Time Periodic Coefficients*. PhD thesis, Graduate School of the University of Maryland at College Park, 1997.

[6] A. Siddiqi, "Identification of the harmonic transfer functions of a helicopter rotor," Master's thesis, Massachusetts Institute of Technology, 2001.

[7] P. Arcara, S. Bittanti, and M. Lovera, "Active control of vibrations in helicopters by periodic optimal control," in *Control Applications, 1997., Proceedings of the 1997 IEEE International Conference on*, pp. 730–735, IEEE, 1997.

[8] M. W. Sracic and M. S. Allen, "Method for identifying models of nonlinear systems using linear time periodic approximations," *Mechanical Systems and Signal Processing*, vol. 25, no. 7, pp. 2705–2721, 2011.

[9] E. Mollerstedt and B. Bernhardsson, "A harmonic transfer function model for a diode converter train," in *Power Engineering Society Winter Meeting, 2000. IEEE*, vol. 2, pp. 957–962, IEEE, 2000.

[10] J. B. Dingwell and J. P. Cusumano, "Nonlinear time series analysis of normal and pathological human walking," *Chaos: An Interdisciplinary Journal of Nonlinear Science*, vol. 10, no. 4, pp. 848–863, 2000.

[11] I. Uyanik, M. M. Ankarali, N. J. Cowan, U. Saranli, and Ö. Morgül, "Identification of a vertical hopping robot model via harmonic transfer functions," *Transactions of the Institute of Measurement and Control*, vol. 38, no. 5, pp. 501–511, 2016.

[12] E. Möllerstedt, *Dynamic analysis of harmonics in electrical systems*. PhD thesis, Lund Institute of Technology, 2000.

[13] N. M. Wereley, *Analysis and control of linear periodically time varying systems*. PhD thesis, Massachusetts Institute of Technology, 1990.

[14] I. Uyanik, *Identification of legged locomotion via model-based and data-driven approaches*. PhD thesis, Bilkent University, 2017.

[15] M. Verhaegen and X. Yu, "A class of subspace model identification algorithms to identify periodically and arbitrarily time-varying systems," *Automatica*, vol. 31, no. 2, pp. 201–216, 1995.

[16] F. Felici, J.-W. Van Wingerden, and M. Verhaegen, "Subspace identification of mimo lpv systems using a periodic scheduling sequence," *Automatica*, vol. 43, no. 10, pp. 1684–1697, 2007.

[17] K. Liu, "Identification of linear time-varying systems," *Journal of Sound and Vibration*, vol. 206, no. 4, pp. 487–505, 1997.

[18] I. Uyanik, U. Saranli, Ö. Morgül, and M. M. Ankarali, "Parametric identification of hybrid linear-time-periodic systems," *IFAC-PapersOnLine*, vol. 49, no. 9, pp. 7–12, 2016.

[19] R. Pintelon and J. Schoukens, *System identification: a frequency domain approach*. John Wiley & Sons, 2012.

[20] S. R. Hall and N. M. Wereley, "Generalized nyquist stability criterion for linear time periodic systems," in *American Control Conference, 1990*, pp. 1518–1525, IEEE, 1990.

[21] J. Zhou and T. Hagiwara, "Generalized nyquist criterion of continuous-time periodic systems and its implementation (i): theoretic results," in *SICE 2002. Proceedings of the 41st SICE Annual Conference*, vol. 3, pp. 1700–1705, IEEE, 2002.

[22] C. Jakobsen, J. Camino, and F. Santos, "Rotor-blade vibration control using a periodic lqr controller," *Proceeding Series of the Brazilian Society of Computational and Applied Mathematics*, vol. 1, no. 1, 2013.

[23] R. MacKillip, "Periodic control of the individual-blade-control helicopter rotor," in *10th European Rotorcraft Forum*, The Hague, 1984.

[24] G. Floquet, "Sur les équations différentielles linéaires à coefficients périodiques," in *Annales scientifiques de l'École normale supérieure*, vol. 12, pp. 47–88, 1883.

[25] D. Owens, L. M. Li, and S. P. Banks, "Multi-periodic repetitive control system: a lyapunov stability analysis for mimo systems," *International Journal of Control*, vol. 77, no. 5, pp. 504–515, 2004.

[26] G. W. Hill, "On the part of the motion of the lunar perigee which is a function of the mean motions of the sun and moon," *Acta Mathematica*, vol. 8, no. 1, pp. 1–36, 1886.

[27] B. D. Anderson and J. B. Moore, *Optimal control: linear quadratic methods*. Courier Corporation, 2007.

[28] M. Athans, "The role and use of the stochastic linear-quadratic-gaussian problem in control system design," *IEEE Transactions on Automatic Control*, vol. 16, no. 6, pp. 529–552, 1971.

[29] R. Z. Scapini, L. V. Bellinaso, and L. Michels, "Stability analysis of half-bridge rectifier employing ltp approach," in *IECON 2012-38th Annual Conference on IEEE Industrial Electronics Society*, pp. 780–785, IEEE, 2012.

[30] L. V. Bellinaso, R. Z. Scapini, and L. Michels, "Modeling and analysis of single phase full-bridge pfc boost rectifier using the ltp approach," in *Power Electronics Conference (COBEP), 2011 Brazilian*, pp. 93–100, IEEE, 2011.

[31] E. Mollerstedt and B. Bernhardsson, "Out of control because of harmonics-an analysis of the harmonic response of an inverter locomotive," *IEEE Control Systems*, vol. 20, no. 4, pp. 70–81, 2000.

[32] M. S. Allen, "Frequency-domain identification of linear time-periodic systems using LTI techniques," *Journal of Computational and Nonlinear Dynamics*, vol. 4, no. 4, p. 041004, 2009.

[33] D. Logan, T. Kiemel, and J. J. Jeka, "Using a system identification approach to investigate subtask control during human locomotion," *Frontiers in Computational Neuroscience*, vol. 10, 2016.

[34] H. Sandberg, E. Mollerstedt, *et al.*, "Frequency-domain analysis of linear time-periodic systems," *IEEE Transactions on Automatic Control*, vol. 50, no. 12, pp. 1971–1983, 2005.

[35] S. Bittanti, G. Fronza, and G. Guardabassi, "Periodic control: A frequency domain approach," *IEEE Transactions on Automatic Control*, vol. 18, no. 1, pp. 33–38, 1973.

[36] N. M. Wereley and S. R. Hall, "Frequency response of linear time periodic systems," in *Proceedings of the IEEE International Conference on Decision and Control*, pp. 3650–3655, IEEE, 1990.

[37] D. A. Peters and K. H. Hohenemser, "Application of the floquet transition matrix to problems of lifting rotor stability," *Journal of the American Helicopter Society*, vol. 16, no. 2, pp. 25–33, 1971.

[38] I. Uyanik, U. Saranli, M. M. Ankarali, and Ö. Morgül, "Frequency domain subspace identification of linear time periodic (LTP) systems," *IEEE Transactions on Automatic Control*, 2017. Under Review.

[39] L. A. Zadeh and C. A. Deoser, *Linear system theory*. Robert E. Krieger Publishing Company Huntington, 1976.

[40] M. Farkas, *Periodic motions*, vol. 104. Springer Science & Business Media, 2013.

[41] I. Uyanik, M. M. Ankarali, N. J. Cowan, Ö. Morgül, and U. Saranli, "Toward data-driven models of legged locomotion using harmonic transfer functions," in *Proceedings of the IEEE International Conference on Advanced Robotics*, pp. 357–362, IEEE, 2015.

[42] R. Grover and P. Y. Hwang, "Introduction to random signals and applied kalman filtering," *Wiley, New York*, 1992.

[43] S. J. Shin, C. E. Cesnik, and S. R. Hall, "System identification technique for active helicopter rotors," *Journal of Intelligent Material Systems and Structures*, vol. 16, no. 11-12, pp. 1025–1038, 2005.

[44] E. Louarroudi, R. Pintelon, J. Lataire, and G. Vandersteen, "Estimation of nonparametric harmonic transfer functions for linear periodically time-varying systems using periodic excitations," in *Proceedings of the IEEE Instrumentation and Measurement Technology Conference*, pp. 1–6, IEEE, 2011.

[45] M. M. Ankarali and N. J. Cowan, "System identification of rhythmic hybrid dynamical systems via discrete time harmonic transfer functions," in *Proceedings of the IEEE International Conference on Decision and Control*, pp. 1017–1022, IEEE, 2014.

[46] I. Uyanik, Ö. Morgül, and U. Saranli, "Experimental validation of a feedforward predictor for the spring-loaded inverted pendulum template," *IEEE Transactions on Robotics*, vol. 31, no. 1, pp. 208–216, 2015.

[47] I. Uyanik, M. M. Ankarali, N. J. Cowan, U. Saranli, Ö. Morgül, and H. Özbay, "Independent estimation of input and measurement delays for a hybrid vertical spring-mass-damper via harmonic transfer functions," *IFAC-PapersOnLine*, vol. 48, no. 12, pp. 298–303, 2015.

[48] I. Uyanik, "Adaptive control of a one-legged hopping robot through dynamically embedded spring-loaded inverted pendulum template," Master's thesis, Bilkent University, 2011.

[49] J. A. Richards, *Analysis of periodically time-varying systems*. Springer Science & Business Media, 2012.

[50] D. T. Sheu, *Effects of tower motion on the dynamic response of windmill rotor*. Massachusetts Institute of Technology, Department of Aeronautics and Astronautics, Aeroelastic and Structures Research Laboratory, 1978.

[51] P. Friedmann, C. Hammond, and T.-H. Woo, "Efficient numerical treatment of periodic systems with application to stability problems," *International Journal for Numerical Methods in Engineering*, vol. 11, no. 7, pp. 1117–1136, 1977.

[52] H. Nyquist, "Regeneration theory," *Bell Labs Technical Journal*, vol. 11, no. 1, pp. 126–147, 1932.

[53] J. F. Barmanj and J. KATZENELSON §, "A generalized nyquist-type stability criterion for multivariable feedback systems," *International Journal of Control*, vol. 20, no. 4, pp. 593–622, 1974.

[54] A. G. MacFarlane and I. Postlethwaite, "The generalized nyquist stability criterion and multivariable root loci," *International Journal of Control*, vol. 25, no. 1, pp. 81–127, 1977.

[55] C. Desoer and Y.-T. Wang, "On the generalized nyquist stability criterion," *IEEE Transactions on Automatic Control*, vol. 25, no. 2, pp. 187–196, 1980.

[56] I. Panardo, "Stability of periodic systems and floquet theory," Master's thesis, Universita Degli Studi Di Padova, 2014.

[57] X. Wang and J. K. Hale, "On monodromy matrix computation," *Computer Methods in Applied Mechanics and Engineering*, vol. 190, no. 18, pp. 2263–2275, 2001.

[58] J. Zhou and T. Hagiwara, "Generalized nyquist criterion of continuous-time periodic systems and its implementation (ii): numerical computations and convergence," in *SICE 2002. Proceedings of the 41st SICE Annual Conference*, vol. 3, pp. 1706–1709, IEEE, 2002.

[59] S. W. Su, B. D. Anderson, and T. S. Brinsmead, "Constant disturbance rejection and zero steady state tracking error for nonlinear systems design," *Applied and Computational Control, Signals, and Circuits*, pp. 1–30, 2001.

[60] M. Burger, *Disturbance Rejection using Conditional Integrators: Applications to path manoeuvring under environmental disturbances for single vessels and vessel formations.* PhD thesis, Norwegian University of Science and Technology, 2011.